

A comprehensive cosmographic analysis by Markov Chain Method

S. Capozziello,

*Dipartimento di Scienze Fisiche, Università degli Studi di Napoli "Federico II" and INFN,
Sezione di Napoli, Complesso Universitario di Monte S. Angelo, Via Cinthia, Edificio N, 80126 Napoli, Italy*

R. Lazkoz, and V. Salzano,

*Fisika Teorikoaren eta Zientziaren Historia Saila, Zientzia eta Teknologia Fakultatea,
Euskal Herriko Unibertsitatea, 644 Posta Kutxatila, 48080 Bilbao, Spain*

We study the possibility to extract model independent information about the dynamics of the universe by using Cosmography. We intend to explore it systematically, to learn about its limitations and its real possibilities. Here we are sticking to the series expansion approach on which Cosmography is based. We apply it to different data sets: Supernovae Type Ia (SNeIa), Hubble parameter extracted from differential galaxy ages, Gamma Ray Bursts (GRBs) and the Baryon Acoustic Oscillations (BAO) data. We go beyond past results in the literature extending the series expansion up to the fourth order in the scale factor, which implies the analysis of the deceleration, q_0 , the jerk, j_0 and the snap, s_0 . We use the Markov Chain Monte Carlo Method (MCMC) to analyze the data statistically. We also try to relate direct results from Cosmography to dark energy (DE) dynamical models parameterized by the Chevalier-Polarski-Linder (CPL) model, extracting clues about the matter content and the dark energy parameters. The main results are: *a.* even if relying on a mathematical approximate assumption such as the scale factor series expansion in terms of time, cosmography can be extremely useful in assessing dynamical properties of the Universe; *b.* the deceleration parameter clearly confirms the present acceleration phase; *c.* the MCMC method can help giving narrower constraints in parameter estimation, in particular for higher order cosmographic parameters (the jerk and the snap), with respect to the literature; *d.* both the estimation of the jerk and the DE parameters, reflect the possibility of a deviation from the Λ CDM cosmological model.

PACS numbers: 04.50.-h, 98.80.-k, 98.80.Es

I. INTRODUCTION

Cosmography is a branch of cosmology which has not been explored so much yet in spite of its promising prospects towards a deeper understanding of the acceleration of the universe. Thus, there remain caveats to be filled and misunderstandings to be rectified before one can take full advantage of the possibilities offered by Cosmography.

This approach proceeds by making minimal dynamical assumptions, namely, it does not assume any particular form of the Friedmann equations and only relies on the assumption that the spacetime geometry is well described on large scales by the Robertson-Walker metric. This makes cosmography fully model and setting independent, in the sense that it is only at the late stages of interpretation of the results offered by this approach that one has to care for the theoretical framework in which the conclusions fit best (dark energy, dark gravity, modified gravity, etc.).

This is clearly important, for instance, when one attempts at comparing the Λ CDM model (or any dark energy model) with alternative theories of gravity (such as $f(R)$ gravity). In the traditional approach a parameterized model is assumed at the beginning, and then, by contrasting it against the data, it is possible to check its viability and to constrain its characterizing parameters. But this approach is clearly a model dependent one so that some doubts always remain on the validity of

the constraints on derived quantities as the present day values of the deceleration parameter and the age of the universe, just to mention a couple of them. Conversely, the constraints that one can infer from cosmography are more universal since they are completely model-free. If well understood and analyzed in full details, weighting its pros and cons, results from Cosmography can be rightly considered as milestones in the study of properties of universe dynamics, which any theoretical model has to consider and satisfy, and can help pointing in the right direction in connection with the properties of the Universe.

Of course, everything is not so clearly cut. The fundamental rule of cosmography is based on the series expansion of the scale factor, $a(t)$. From it one obtains the cosmographic parameters usually referred to as the *Hubble* (H), *deceleration* (q), *jerk* (j), *snap* (s) and *lerk* (l) parameters, which we define below. However, the series of $a(t)$ places difficulties almost from the very beginning. As discussed in [1], there are two main problems when working with series expansions: the convergence and the truncation of the series. Those authors show it is possible to solve the convergence problem defining a new redshift variable, the so called *y-redshift*:

$$z \rightarrow y = \frac{z}{1+z} . \quad (1)$$

For a series expansion in the classical z -redshift the convergence radius is equal to 1. This represents a drawback

when one wants to extend the application of cosmography to redshift $z > 1$, which is not such a big past extension, if we consider that current supernovae data go up to $z = 1.4$, or that the CMB analysis involves the decoupling redshift $z \approx 1089$. It would be pleasant to be able to work correctly at least up to the highest redshift demanded by the observational data set one wants to use.

The y -redshift could potentially solve this problem because the z -interval $[0, \infty]$ corresponds to the y -interval $[0, 1]$, so that we are mainly inside the convergence interval of the series, even for CMB data ($z = 1089 \rightarrow y = 0.999$). So, in principle, we could extend the series up to the decoupling redshift value, and one could place CMB related constraints within the cosmographic approach. Unfortunately, some problems arise and we will discuss them below. Leaving aside this limitation, the possibilities offered by the y -redshift can be considered as a step in the right direction, because, obviously, defining a new redshift does not change the physical content of the data.

But the problem of the truncation of the series is not solved; of course, we expect that for low redshifts a low order series expansion will work well, while for higher redshifts it is likely that higher order expansions of any physical quantity of relevance will be required. But, is this true? And what is the good order for any redshift? Is there an even approximate relation which correlates redshift with series order?

This paper represents an improvement in this direction. As considering a higher order of expansion enforces taking into account more free parameters, it seems a priori it will be difficult to obtain tight constraints on them if the discriminating power of the data sets used is weak or not fully exploited statistically. Despite this, we successfully put bounds on the parameters of the third order series in a statistically consistent way, and so make a considerable improvement with respect to [2], where for the same redshift extent the authors only managed to put constraints on the coefficients of a second order series. This is one of the major contributions of our paper.

In addition, there is another matter on which this paper enhances the worth of the cosmographic approach: the values and the errors of the cosmographic parameters. Estimations of that sort can be found in the literature, not only in [2], but also in [3] and [4]. While the former used supernovae data, in related works like [5–9] one can find theoretical estimations (in the context of $f(R)$ theories in both metric and Palatini approaches) which could be related to estimations from observational data. Some recent contributions to this topic are the works [10, 11], where gamma ray burst data have been used. Here we analyze at the same time data from SNeIa and GRBs, and combine them with a sample of Hubble parameters values extracted by means of the differential galaxy ages, and BAO data. The use of the Hubble parameter data, in particular, introduces additional advantages we will refer to later.

The main problem with earlier contributions to the

topic is that the error bars obtained were considerably large. Due to this fact, the statistical conclusions to be inferred are rather weak and, in consequence, they hardly provide valid priors for future analysis. For example, from [4] we have $q_0 = -0.90 \pm 0.65$, $j_0 = 2.7 \pm 6.7$, $s_0 = 36.5 \pm 52.9$, $l_0 = 142.7 \pm 320$; some of the relative errors are as high as about a 200% (as usual, the 0 subindex denotes the $z = 0$ values of the parameters). Now, we can expect that errors on the coefficients will get bigger when higher order expansions are considered. As those parameters are correlated among them, errors in the low order series coefficients propagate to the additional coefficients included in the higher order series. If these errors turn out to be big, the positive aspects of cosmography will vanish. For instance, if the error on q_0 allows for a positive value of the deceleration parameter in the 3σ confidence interval, it will not be so obvious that the Universe is accelerating (see again [2]). Moreover, the Λ CDM model enforces $j_0 = 1$ (this can be easily derived from the definition of j_0 , which is to be found in § (III)); but if the error bar is as big as reported above (from [4]), it will not be possible to confront this model with competing ones.

Given those problems we have just discussed, an important question arises: is it not possible to give narrower statistical constraints? To this end we apply a Markov Chain Monte Carlo (MCMC) method: it allows us obtaining marginalized likelihoods on the series coefficients from which we infer rather tight constraints on those parameters. The reason for this considerable improvement with respect to earlier works is that in our code we have implemented several controls which give us power over any physical requirement we expect from our theoretical apparatus. Actually, setting restrictions on the Hubble parameter is possible because we use data related to this quantity that reveal to allow a considerable improvement in the quality of constraints.

We have organized the paper as follows: in § (II) and Appendix) we define the cosmographic parameters and give all the relations needed; in § (III) we describe some caveats that have to be taken in mind when working with Cosmography; in § (IV) we describe the observational data used for the analysis; in § (V) and § (VI) we present our main results and discuss their meaning and consequences; finally, in § (VII) we summarize.

II. COSMOGRAPHIC PARAMETERS

The key rule in cosmography is the Taylor series expansion of the scale factor with respect to the cosmic time. To this aim, it is convenient to introduce the following functions:

$$H(t) = \frac{1}{a} \frac{da}{dt},$$

$$q(t) = -\frac{1}{a} \frac{d^2a}{dt^2} \frac{1}{H^2},$$

$$\begin{aligned}
j(t) &= \frac{1}{a} \frac{d^3 a}{dt^3} \frac{1}{H^3}, \\
s(t) &= \frac{1}{a} \frac{d^4 a}{dt^4} \frac{1}{H^4}, \\
l(t) &= \frac{1}{a} \frac{d^5 a}{dt^5} \frac{1}{H^5}.
\end{aligned} \tag{2}$$

They are usually referred to as the *Hubble*, *deceleration*, *jerk*, *snap* and *lerk* parameters, respectively (see [12] for an historical account of these names). Using these definitions it is easy to write the fifth order Taylor expansion of the scale factor:

$$\begin{aligned}
\frac{a(t)}{a(t_0)} &= 1 + H_0(t - t_0) - \frac{q_0}{2} H_0^2(t - t_0)^2 + \frac{j_0}{3!} H_0^3(t - t_0)^3 \\
&+ \frac{s_0}{4!} H_0^4(t - t_0)^4 + \frac{l_0}{5!} H_0^5(t - t_0)^5 + O[(t - t_0)^6] \tag{3}
\end{aligned}$$

with t_0 being the current age of the universe. Note that Eq. (3) is also the fifth order expansion of $(1 + z)^{-1}$, as the definition for the redshift z is $z := a(t_0)/a(t) - 1$. This is what we need for developing the cosmographic apparatus; for sake of clearness we remind all the detailed calculations to the appendix section, while giving here only the main results.

A. Luminosity distance series

Since we are going to use SNeIa and GRBs data, it will be useful to give the Taylor series of the expansion of the distance modulus, which is the quantity about which those observational data typically inform. The final expression for the distance modulus based on the Hubble free luminosity distance (Eqs. (A5) - (A6)), $\mu(z) = 5 \log_{10} d_L(z) + \mu_0$, is the following:

$$\begin{aligned}
\mu(z) &= \frac{5}{\log 10} (\log z + \mathcal{M}^1 z + \mathcal{M}^2 z^2 + \mathcal{M}^3 z^3 + \mathcal{M}^4 z^4) \\
&+ \mu_0, \tag{4}
\end{aligned}$$

with

$$\begin{aligned}
\mathcal{M}^1 &= -\frac{1}{2} [-1 + q_0], \\
\mathcal{M}^2 &= -\frac{1}{24} [7 - 10q_0 - 9q_0^2 + 4j_0], \\
\mathcal{M}^3 &= \frac{1}{24} [5 - 9q_0 - 16q_0^2 - 10q_0^3 + 7j_0 + 8q_0j_0 + s_0], \\
\mathcal{M}^4 &= \frac{1}{2880} [-469 + 1004q_0 + 2654q_0^2 + 3300q_0^3 + 1575q_0^4 \\
&+ 200j_0^2 - 1148j_0 - 2620q_0j_0 - 1800q_0^2j_0 - 300q_0s_0 \\
&- 324s_0 - 24l_0].
\end{aligned}$$

Of course we have also derived the same relations for the y -redshift, but we relegate them to the appendix.

B. Hubble parameter series

The definition of the luminosity distance given by Eq. (A3), can be presented in this other way:

$$D_L(z) = c (1 + z) \int_0^z dz' \frac{1}{H(z')}. \tag{5}$$

It is interesting to study the possibility of obtaining the same final expression for the distance defined starting from a Taylor series expansion of the Hubble parameter instead of the scale factor, namely:

$$\begin{aligned}
H(z) &= H_0 + \frac{dH}{dz} \Big|_{z=0} z + \frac{1}{2!} \frac{d^2 H}{dz^2} \Big|_{z=0} z^2 + \frac{1}{3!} \frac{d^3 H}{dz^3} \Big|_{z=0} z^3 \\
&+ \frac{1}{4!} \frac{d^4 H}{dz^4} \Big|_{z=0} z^4 + O(z^5). \tag{6}
\end{aligned}$$

This series expansion will be also an important rule in the definition of our Markov chains algorithm given the observational data we use. To compute all the terms of this series we have to keep in mind the derivation rule (for a clearer notation we will suppress the redshift dependence of the Hubble parameter setting $H \equiv H(z)$):

$$\frac{d}{dt} = -(1 + z) H \frac{d}{dz}. \tag{7}$$

It is an easy but cumbersome task to obtain from the latter the higher-order time-derivatives of the Hubble parameter (they are given in § (C)). Then, from the definitions of the cosmographic parameters, Eq. (2), it is easy to demonstrate the following relations:

$$\dot{H} = -H^2(1 + q), \tag{8}$$

$$\ddot{H} = H^3(j + 3q + 2), \tag{9}$$

$$\frac{d^3 H}{dt^3} = H^4 [s - 4j - 3q(q + 4) - 6], \tag{10}$$

$$\begin{aligned}
\frac{d^4 H}{dt^4} &= H^5 [l - 5s + 10(q + 2)j \\
&+ 30(q + 2)q + 24] \tag{11}
\end{aligned}$$

If we convert time-derivatives into derivatives with respect to redshift using Eqs. (7) - (C1) - (C2) - (C3) we have:

$$\frac{dH}{dz} = \frac{H}{1 + z} (1 + q), \tag{12}$$

$$\frac{d^2 H}{dz^2} = \frac{H}{(1 + z)^2} (-q^2 + j), \tag{13}$$

$$\frac{d^3 H}{dz^3} = \frac{H}{(1 + z)^3} (3q^2 + 3q^3 - 4qj - 3j - s), \tag{14}$$

$$\frac{d^4 H}{dz^4} = \frac{H}{(1+z)^4} (-12q^2 - 24q^3 - 15q^4 + 32qj + 25q^2j + 7qs + 12j - 4j^2 + 8s + l) . \quad (15)$$

Exactly the same luminosity distance formula as given in Eq. (A5) can be recovered after a series of steps: after having evaluated Eqs. (12) - (15) at $z = 0$ (namely t_0), we must insert them in Eq. (6), and then insert this one in Eq. (5). Then we must Taylor expand the integration function, integrate it, and we will have reached the final sought result and the coincidence will be complete.

This is all, so far, in what the basic setup is concerned, in the next section we move on to applications of these definitions.

III. SERIES ORDERS COMPARISON

As we have said in the introductory section, the first question we would try to answer is whether there is a relation between the highest expansion order in the Taylor series and the redshift range where this series can be applied. What one could expect is the rough rule that we would need a series expansion truncated at higher orders when increasing up the redshift range. This would be a mathematical requirement, of course. But what about physics, our main interest, and the fit to the Hubble SNeIa diagram; namely, the reproduction of the luminosity distance or its corresponding distance modulus? We have found that the answer seems to be not so obvious.

Let us start by writing some useful relations for successive results. To make the discussion more specific we will use the Chevallier - Polarski - Linder (CPL) ([13],[14]) parametrization:

$$w = w_0 + w_a(1 - a) = w_0 + w_a z(1 + z)^{-1} , \quad (16)$$

so that, in a spatially flat universe filled with cold dark matter and dark energy, the dimensionless Hubble parameter $E(z) = H/H_0$ reads:

$$E^2(z) = \Omega_m(1+z)^3 + \Omega_X(1+z)^{3(1+w_0+w_a)} e^{-\frac{3w_a z}{1+z}} . \quad (17)$$

with $\Omega_X = 1 - \Omega_m$ because of the flatness assumption. In order to determine the cosmographic parameters for such a model, we avoid integrating $H(z)$ to get $a(t)$ by noting that $d/dt = -(1+z)H(z)d/dz$. We can use such a relation to evaluate $(\dot{H}, \ddot{H}, d^3H/dt^3, d^4H/dt^4)$ and convert Eqs. (8) - (11) to redshift derivatives, i.e.:

$$q(z) = \frac{(1+z)}{2H^2(z)} \frac{dH^2(z)}{dz} - 1 ,$$

$$j(z) = \frac{(1+z)^2}{2H^2(z)} \frac{d^2H^2(z)}{dz^2} - \frac{(1+z)}{H^2(z)} \frac{dH^2(z)}{dz} + 1 . \quad (18)$$

For the snap and the lerk the expressions are much longer and involve respectively the third and the fourth order derivatives of $H^2(z)$. We underline that these expressions for cosmographic parameters are exact. Given an

analytical expression for $H(z)$, we can evaluate them at $z = 0$, and solve them with respect to the parameters of interest.

Some algebra finally gives:

$$q_0 = \frac{1}{2} + \frac{3}{2}(1 - \Omega_m)w_0 , \quad (19)$$

$$j_0 = 1 + \frac{3}{2}(1 - \Omega_m) [3w_0(1 + w_0) + w_a] , \quad (20)$$

$$s_0 = -\frac{7}{2} - \frac{33}{4}(1 - \Omega_m)w_a$$

$$- \frac{9}{4}(1 - \Omega_m) [9 + (7 - \Omega_m)w_a] w_0 - \frac{9}{4}(1 - \Omega_m)$$

$$\times (16 - 3\Omega_m)w_0^2 \frac{27}{4}(1 - \Omega_m)(3 - \Omega_m)w_0^3 , \quad (21)$$

$$l_0 = \frac{35}{2} + \frac{1 - \Omega_m}{4} [213 + (7 - \Omega_m)w_a] w_a$$

$$+ \frac{(1 - \Omega_m)}{4} [489 + 9(82 - 21\Omega_m)w_a] w_0$$

$$+ \frac{9}{2}(1 - \Omega_m) \left[67 - 21\Omega_m + \frac{3}{2}(23 - 11\Omega_m)w_a \right] w_0^2$$

$$+ \frac{27}{4}(1 - \Omega_m)(47 - 24\Omega_m)w_0^3$$

$$+ \frac{81}{2}(1 - \Omega_m)(3 - 2\Omega_m)w_0^4 . \quad (22)$$

From Eq. (17) we can derive the exact analytical expression for the Hubble free luminosity distance and the distance modulus. Then, we will compare it with its expression as a cosmographic series, i.e. a series depending on the cosmographic parameters. We have considered the cosmographic series with two (q_0, j_0) , three (q_0, j_0, s_0) and four parameters (q_0, j_0, s_0, l_0) . Of course, from any CPL scenario we will be able to derive the corresponding set of cosmographic parameters using Eqs. (19) - (22).

We have tested two different toy models: a Λ CDM model ($\Omega_m = 0.3$, $w_0 = -1$, $w_a = 0$); and a dynamical dark energy model with $\Omega_m = 0.245$, $w_0 = -0.93$, $w_a = -0.41$ coming from [15]. In Figs. (1) - (2) we show the comparison in the redshift range $0 < z < 2$, which is the range where cosmography has been mainly applied in past works, regarding to the maximum available redshift of the SNeIa surveys used in the literature.

As we can see in Fig. (1), it is not so obvious that the series expanded at higher orders can describe well the underlying Hubble parameter or distance modulus when applying cosmography out of the convergence radius. There we show the relative residuals with respect to the exact CPL functions (i.e. the Hubble parameter and the distance modulus) coming from the different order series in the Λ CDM case. As we can see, inside the redshift convergence radius ($z < 1$) the four-parameter series effectively gives a better approximation to the Hubble parameter and the distance modulus than other orders expansions.

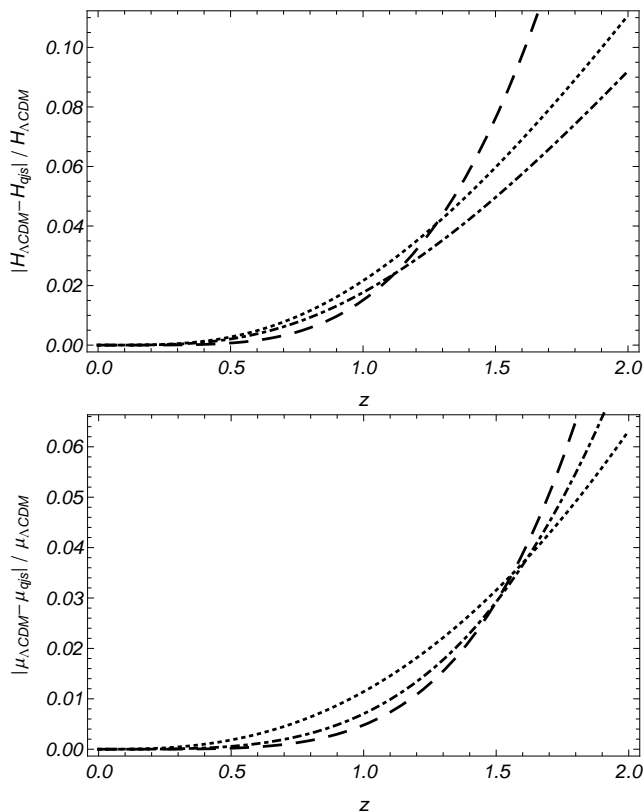


Figure 1. (*Top.*) Residuals between the CPL exact Hubble function and different-order series expansions of the same quantity in the Λ CDM case. The redshift range is $0 < z < 2$. (*Bottom.*) The same as above picture but for distance modulus. One might expect that the value of the denominator, $\mu_{\Lambda\text{CDM}}$, depends on the nuisance parameter μ_0 , i.e. on the value of the Hubble constant, H_0 . But we have checked that changing H_0 in the range $[0.65, 0.75]$, which is large enough to contain all the acceptable physical values of H_0 , does not produce any sensible change in the figures.

But it is also clear that the rough rule (higher redshift, higher order series) is somewhat not followed when out of the convergence interval, namely, above $z = 1$. In this case residuals from the four-parameter expansion grow with redshift faster than the ones coming from the three and two-parameters ones.

The same analysis made with the dynamical model lead to similar final conclusions and adds further interesting caveats which have to be kept in mind when working with cosmography and using its results. Looking at Fig. (2) we can see some consequences from changing the cosmological model:

- the inversion in goodness between the order series expansions even inside the convergence radius. In the $H(z)$ case, we can see that in the Λ CDM model, for $z > 1$, the two and the tree-parameters expansions were quite similar, with a slight preference for the latter one. In the dynamical dark energy model things go different, and the two-parameters

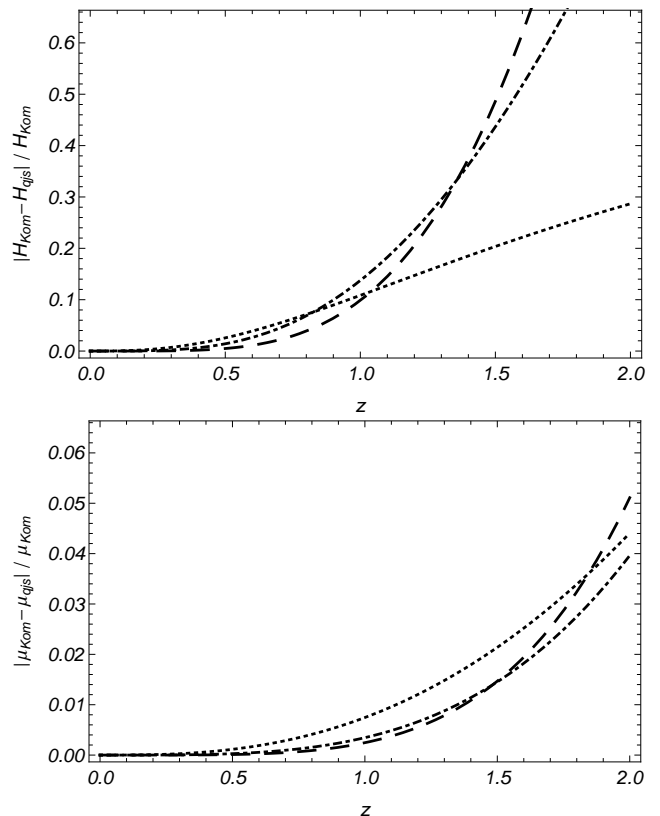


Figure 2. (*Top.*) Residuals between the CPL exact Hubble function and different-order series expansions of the same quantity in the model from [15]. The redshift range is $0 < z < 2$. (*Bottom.*) The same as above picture but for distance modulus.

expansion is strongly preferred;

- different magnitudes for residuals, notably in the Hubble function case, slightly in the distance modulus.

The first point leads us to think about the real effectiveness of cosmography approach as a “*model independent*” one. Cosmography is model independent, of course, starting from its basic assumptions, and the information pieces one can extract from it are model independent too; but data are tracers of a cosmological model.

From the previous considerations it seems that there is an implicit relation between the series expansion and the underlying *unknown* cosmological model which we want to read out from data. If cosmography, by its order series expansion, is sensible enough to detect and discriminate a model against another one, then the choice of working with two, three or four parameters can be critical.

The second consideration is important for defining the main lesson of this section. All the analysis we have done until now could be useless without relating it to the experimental possibilities we have nowadays. Namely: are our present data and their related errors able to make

us distinguish between a two, three, or four-parameter expansion for the measured physical quantities we are working with?

To answer this question we need a look at the data we are going to use. If we consider the data from [16], we see that the relative errors on $H(z)$ range in the interval $[0.10, 0.62]$, which is clearly larger than the residual we have plotted in Figs. (1) - (2). So any possibility to discriminate what the right expansion order is in cosmography is completely out of question. Things are slightly better with the SNeIa data set, which shows relative errors in a range $[0.002, 0.025]$. But even now results have to be taken with a pinch of salt. For example, in the redshift range $z < 1$, SNeIa relative errors are ≤ 0.010 , which means that they are of the same order of the residuals we have found. In this case, we can say we are in a “border-line” situation.

Last but not least, we have done the same analysis working with the y -redshift. In this case we have found out that the higher order series give a better approximation to the exact relation than the lower order ones, which is quite expected, because we are always well inside the convergence radius, i.e. $0 < y < 1$. On the contrary, the most important thing that emerges, is that the y -redshift can be useful only up to a certain redshift. Above a certain limit it cannot be used to constrain the Hubble parameter or distance modulus, for some intrinsic mathematical properties coming from its definition. As it is showed in the Fig. (3), above $y \approx 0.4 \div 0.5$, there is a clear deviation between the series expansions and the exact expression of our physical quantities, larger than observational errors. And the y -redshift series are unable to follow the right trend.

For all these reasons, we have chosen to work in the reminder with second and third order series expansions, giving at most constrains to the deceleration, the jerk and the snap parameters. We have seen that it is impossible to extend the analysis to four parameters, the lerk being completely undetermined.

IV. OBSERVATIONAL TESTS

A. Hubble parameter

Recently in [16] an update of the Hubble parameter $H(z)$ data extracted from differential ages of passively evolving galaxies previously published in [17] was presented. In [18] this method was analyzed and some caveats about its use are exposed; anyway, data in [16] are considered greatly improved with respect of previous ones derived in [17]. Constraining the background evolution of the universe using these data is interesting for several reasons. Firstly, they can be used together with other cosmological tests in order to get useful consistency checks or tighter constraints on models. Secondly, it is well known that detailed and reliable information in the behavior of $H(z)$ is lost when using the luminosity dis-

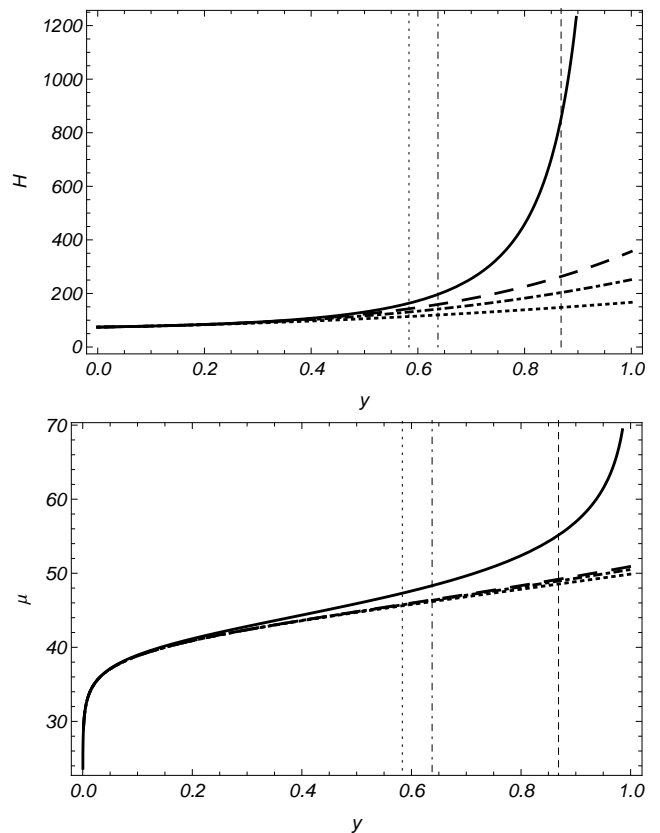


Figure 3. (*Top.*) Hubble parameter in the Λ CDM model. The y -redshift range is $0 < y < 1$. The solid black line is the exact analytical expression; the dashed line is the fourth order series; the dot-dashed line is the third order series; and the dotted line is the second order series. The vertical dotted line is the maximum redshift from SNeIa sample; the vertical dotdashed line is the maximum redshift from Hubble data; the vertical dashed line is the maximum redshift from GRBs sample. (*Bottom.*) The same as above picture but for distance modulus.

tance or the correlated modulus distance. As a result of the integration of this function, the fine details cannot be analyzed and no information can be derived (if there is any information, probing or refuting the previous ones). For this reason, we have chosen to work with this data set: any refinement in the Hubble parameter could give important details.

The Hubble parameter dependence on the differential age of the Universe in terms of redshift is given by

$$H(z) = -\frac{1}{1+z} \frac{dz}{dt}. \quad (23)$$

Thus, $H(z)$ can be determined from measurements of dt/dz . As reported in [16], [17], [19] and [20], values of dt/dz can be computed using absolute ages of passively evolving galaxies.

The galaxy spectral data used by [16] come from observations of bright cluster galaxies done with the Keck/LRIS instrument (see [21] for a detailed description

of the observations, reductions and the catalog of all the measured redshifts). The purposely planned Keck-survey observations have been extended with other datasets: SDSS improvements in calibration available in the Public Data Release 6 (DR6) have been applied to data in [20]; the SPICES infrared-selected galaxies sample in [22]; and the VVDIS survey by the VLT/ESO telescope in [23].

The authors of these references bin together galaxies with a redshift separation which is small enough so that the galaxies in the bin have roughly the same age; then, they calculate age differences between bins which have a small age difference which is at the same time larger than the error in the age itself ([16]). The outcome of this process is a set of 12 values of the Hubble parameter versus redshift. A particularly nice feature of this test is that the sensitivity of differential ages to systematic error is lower than in the case of absolute ages ([24]).

Observed values of $H(z)$ can be used to estimate cosmographic parameters by minimizing the quantity

$$\chi_{\text{H}}^2(H_0, \{\theta_i\}) = \sum_{j=1}^{12} \frac{(H(z_j; \{\theta_i\}) - H_{\text{obs}}(z_j))^2}{\sigma_{\text{H}}^2(z_j)} \quad (24)$$

where $H_0 \doteq 100 h$ will be fixed as $h = 0.742$ ([25]), while θ_i is the vector of model parameters, namely in our case $\theta_i = (q_0, j_0, s_0)$.

To minimize the χ^2 function we will use Markov Chain Monte Carlo (MCMC) methods (fully described in [26], [27], [28] and references therein) testing their convergence with the method developed and fully described in [29].

B. Supernovae

We use the most updated SNeIa sample we have now, the Union2 sample described in [30]. The Union2 SNeIa compilation is the result of a new low-redshift nearby-Hubble-flow SNeIa and new analysis procedures to work with several heterogeneous SNeIa compilations. It includes the Union data set from [31] with six SNeIa first presented in [30], with SNeIa from [32], the low- z and the intermediate- z data from [33] and [34] respectively. After various selection cuts were applied in order to create a homogeneous and high signal-to-noise data set, we have final 557 SNeIa events distributed over the redshift interval $0.015 \leq z \leq 1.4$.

The statistical analysis of Union2 SNeIa sample rest on the definition of the distance modulus,

$$\mu(z_j) = 5 \log_{10}(d_L(z_j, \{\theta_i\})) + \mu_0 \quad (25)$$

where $d_L(z_j, \{\theta_i\})$ is the Hubble free luminosity distance, Eq. (A5), expressed as a series and depending on the cosmographic parameters, $\theta_i = (q_0, j_0, s_0)$. The best fits were obtained by minimizing the quantity

$$\chi_{\text{SN}}^2(\mu_0, \{\theta_i\}) = \sum_{j=1}^{557} \frac{(\mu(z_j; \mu_0, \{\theta_i\}) - \mu_{\text{obs}}(z_j))^2}{\sigma_{\mu,j}^2} \quad (26)$$

where the $\sigma_{\mu,j}^2$ are the measurement variances. The nuisance parameter μ_0 encodes the Hubble constant and the absolute magnitude M , and has to be marginalized over. Giving the heterogeneous origin of Union data set, and the procedures described in [31] for reducing data, we have worked with an alternative version of Eq. (26), which consists in minimizing the quantity

$$\tilde{\chi}_{\text{SN}}^2(\{\theta_i\}) = c_1 - \frac{c_2^2}{c_3} \quad (27)$$

with respect to the other parameters. Here

$$c_1 = \sum_{j=1}^{557} \frac{(\mu(z_j; \mu_0 = 0, \{\theta_i\}) - \mu_{\text{obs}}(z_j))^2}{\sigma_{\mu,j}^2}, \quad (28)$$

$$c_2 = \sum_{j=1}^{557} \frac{(\mu(z_j; \mu_0 = 0, \{\theta_i\}) - \mu_{\text{obs}}(z_j))}{\sigma_{\mu,j}^2}, \quad (29)$$

$$c_3 = \sum_{j=1}^{557} \frac{1}{\sigma_{\mu,j}^2}. \quad (30)$$

It is trivial to see that $\tilde{\chi}_{\text{SN}}^2$ is just a version of χ_{SN}^2 , minimized with respect to μ_0 . To that end it suffices to notice that

$$\chi_{\text{SN}}^2(\mu_0, \{\theta_i\}) = c_1 - 2c_2\mu_0 + c_3\mu_0^2 \quad (31)$$

which clearly becomes minimum for $\mu_0 = c_2/c_3$, and so we can see $\tilde{\chi}_{\text{SN}}^2 \equiv \chi_{\text{SN}}^2(\mu_0 = 0, \{\theta_i\})$. Furthermore, one can check that the difference between χ_{SN}^2 and $\tilde{\chi}_{\text{SN}}^2$ is negligible.

C. Gamma Ray Bursts

Working and interpreting results from a GRBs analysis is not an easy task, being the errors on their observable quantities much larger than those ones for SNeIa, and being their source mechanism still not well understood. For this reason choosing a good GRBs sample is crucial; we have chosen to work with the sample described in [35]. There the authors perform a new calibration procedure on the widely used GRBs sample from [36] which perfectly matches our requirements for using them with cosmography. The possibility of a joint analysis of SNeIa and GRBs is strictly related to the building of a Hubble diagram for GRBs too, being this extremely difficult because of GRBs are not standard candles as SNeIa. To create an Hubble diagram for GRBs, one has to look for a correlation between a distance dependent quantity and a directly observable property. Starting from some of the many correlations that have been suggested in the last years, [36] created a sample of 69 GRBs in the redshift range $0.17 < z < 6.6$ whose Hubble diagram is well settled.

In [35] the authors have updated such a sample in many aspects, the main one being the test of a new method for the calibration of GRBs based on the assumption of none *a priori* cosmological model. Such a model independent calibration is built on the idea that SNeIa and GRBs at the same redshift should exhibit the same distance modulus. In this way, interpolating the SNeIa Hubble diagram gives the value of $\mu(z)$ for a sub-sample of GRBs which lies in the same redshift range. This sub-sample can be finally used for calibrating the well known GRBs correlations and, assuming that this calibration is redshift independent, it can be extended to high redshift GRBs. With this procedure, in [35] the authors were able to convert the [36] sample to a new one, with the same number of objects but with SNeIa-calibrated GRBs distance modulus. These data can then be used for minimizing the corresponding χ^2 :

$$\chi_{\text{GRB}}^2(\{\theta_i\}) = \sum_{j=1}^{69} \frac{(\mu(z_j; \{\theta_i\}) - \mu_{\text{obs}}(z_j))^2}{\sigma_{\mu,j}^2}. \quad (32)$$

D. Baryonic Acoustic Oscillations

In [37] the authors analyze the clustering of galaxies within the spectroscopic Sloan Digital Sky Survey (SDSS) Data Release 7 (DR7) galaxy sample, including both the Luminous Red Galaxy (LRG) and Main samples, and also the 2-degree Field Galaxy Redshift Survey (2dFGRS) data. In total, the sample comprises 893319 galaxies over 9100 deg². Baryon Acoustic Oscillations are observed in power spectra measured for different slices in redshift; this allows constraining the distance-redshift relation at multiple epochs. A distance measure at redshift $z = 0.275$ was achieved; but what is more important for our application of cosmography is the almost independent constraint on the ratio of distances,

$$\mathcal{B} = \frac{D_V(0.35)}{D_V(0.2)} = 1.736 \pm 0.065, \quad (33)$$

which is consistent at 1.1σ level with the best fit Λ CDM model obtained when combining the $z = 0.275$ derived distance constraint with the WMAP 5-year data. This measurement is particularly well suited for our purpose, because without it we could not apply BAO constraints on cosmographic approach. The usually derived distance measure from BAO are in the form $r_s(z_d)/D_V$, where $r_s(z_d)$ is the comoving sound horizon at the baryon drag epoch, while D_V is defined as:

$$D_V(z_{\text{BAO}}) = \left[\left(\int_0^{z_{\text{BAO}}} \frac{cdz}{H(z)} \right)^2 \frac{cz_{\text{BAO}}}{H(z_{\text{BAO}})} \right]^{1/3} \quad (34)$$

with $H(z)$ the Hubble parameter. It is clearly obvious that the sound horizon quantity is incompatible with cosmography, being it evaluated at the drag epoch redshift which is $z \approx 1000$, well out of the possible redshift

applicability range of cosmography. On the contrary, the quantity D_V can be easily used for cosmography by substituting for $H(z)$ the appropriate series expression and evaluating it at $z = 0.2$ and 0.35 , well inside the convergence redshift radius of cosmographic series. The quantity \mathcal{B} can then be used for estimating cosmographic parameters by minimizing the quantity

$$\chi_{\text{BAO}}^2(\{\theta_i\}) = \frac{(\mathcal{B}(\{\theta_i\}) - \mathcal{B}_{\text{obs}})^2}{\sigma_{\mathcal{B}}^2}. \quad (35)$$

V. COSMOGRAPHIC ANALYSIS

As said in the previous sections, we have used an MCMC algorithm to perform the analysis of the multi-dimensional space of the cosmographic parameters.

Our main purpose is to explore the possibility of obtaining better constraints on the cosmographic parameters than offered by the literature. This is our motivation to use MCMC methods; as opposed to the approaches used in past examples in the same field, our choice offers the interesting possibility to introduce and manage easily possible physical constraints, thus making it possible to discover underlying relations and to realize a systematic report of the results.

A. Preliminary discussion

First of all, we try to answer a question: are there any physical constraints that can be imposed as priors to our fitting procedure? If yes: how do these constraints work on the estimation of parameters?

The accuracy of the fitting parameters is of course a property derived from the likelihood function and it is quite independent of the method used for its maximization. The point that we want to investigate here is if there is any physical reasonable prior that can be introduced in such analysis for reducing the historically large uncertainties on cosmographic parameters (as described in the introduction). While a great part of these uncertainties surely depend on the series approach which cosmography is based on, we think that probably one could improve the analysis imposing some physical basic and general requirements. For example: does it make any sense to perform a minimization of χ^2 without considering if the best fit parameters give well based physical information, i.e. without considering how physics is mapped in the parameter space (in our case: cosmographic parameter space)?

This is a matter of great importance (and also their strong point in our idea) just while using statistical methods like the MCMC: they are based on an algorithm that moves “randomly” in the parameter space: do all the points (even around the minimum χ^2 location) tested by this algorithm satisfy some general physical requirements, as a positive d_L or a positive H^2 ? These questions

would be of course useless if we were working with exact analytical expressions but, as long as cosmography is built on series expansions, we think it is necessary to analyze this aspect.

As we will show below, even if we will be able to sensibly reduce uncertainties on cosmographic parameters, other problems arise (as, for example, the dependence on the maximum order series expansion, and on the data redshift range) that are intrinsic to the cosmographic apparatus.

The main quantities we are going to fit are the Hubble parameter and the distance modulus; we are quite sure that these quantities will be physically well-based in the best fit location and around it. However, we have to take into account also quantities that are not tested directly. For example, eventual constraints have to be given to the series expansions of $H^2(z)$ and $d_L(z)$. The most general and obvious limitation is the positiveness of these two functions: for H^2 it is a natural mathematical property; and the same consideration is true for d_L , this being a distance. At the same time there is not a direct connection between the positiveness of H and d_L : it is possible to have an $H(z)$ function with varying signature, for example a sinusoidal one, and having a positive definite luminosity distance. We have also verified that, obviously, when fitting models in the redshift range of our data we automatically get a definite positive $H(z)$, at least in the prescribed redshift range (thus excluding a bounce).

Then another question arises naturally: does it make any sense to extend the priors (in our case the positiveness of the physical functions) to any range of redshift well beyond the convergence radius of the series? The answer to this question is not so simple. Since we are working with a truncated series expression we have to impose a “*minimum requirement*” for the positivity of our functions: it ranges only in the limited convergence redshift interval, $0 < z < 1$ or in the redshift range defined by the used data sets. For this reason we also perform a cosmographic analysis both using the full (in a redshift sense) data samples and a cut sub-sample limited to $z > 1$. We also test what happens when extending positivity to all the possible redshift values, namely $z > 0$ even if this would be rigorously right only if we were working with *exact* analytical functions, and to the maximum redshift value coming from any observational sample.

Instead, in the y-redshift, things are different: this quantity spans all the physical distances we are interested in, and it remains always inside the series convergence radius, as $0 < y < 1$. So we can impose positivity on all the y-redshift interval without having forced final results and loss of information due to this choice. Anyway we also test results when the y-redshift is constrained to the range corresponding to the relative z-redshift range for comparing results.

We have also found it is possible to add another constraint: the requirement that Ω_m be positive and smaller than unity. Using the procedure we will describe in next section, where we will compare our cosmographic

analysis with dark energy models described by the CPL parametrization, it turns out that Ω_m is a function of the cosmographic parameters. In the two dimensional case we have

$$\Omega_m(q_0, j_0) = \frac{2(j_0 - q_0 - 2q_0^2)}{1 + 2j_0 - 6q_0}, \quad (36)$$

while in the three dimensional case the expression becomes quite longer, so we omit it for the sake of simplicity. Clearly, the above mentioned constraint on Ω_m can be enforced while running the MCMC algorithm.

At the end, our priors are:

- $d_L(z) > 0$;
- $H^2(z) > 0$;
- $0 < \Omega_m < 1$,

applied on both z and y redshift ranges.

Finally, for fully understanding and comparing our results with literature, it is order now to underline the different use we have made of the jerk as compared to previous references. In [1] and [10], the quantity $j_0 + \Omega_0$ was estimated, where

$$\Omega_0 = 1 + \frac{kc^2}{H_0^2 a_0^2}. \quad (37)$$

As stated in § (VII), in our case the spatial curvature is assumed to be $k = 0$ so that we can derive j_0 values also from other different works. Of course when comparing our results to these ones, we have to consider that in those cases error bars correspond to the composite quantity $j_0 + \Omega_0$. But we are confident that, considering independent estimations of the curvature parameter and its related error, the largest contribution to errors is mainly attributable to the jerk parameter. On the other side, in [5], [38] and [39] the jerk parameter has the same definition as we use. Finally, in [10] GRBs were the only data used (instead of SNeIa).

B. z-redshift

Finally, if we consider the analysis with the common definition of z-redshift, looking at Tables (I) - (II) we can summarize the main results as follows:

- with two cosmographic parameters, working with cut subsamples, namely considering only data with $z < 1$, always gives better results than using the complete sample and results are mostly uniform. This is a direct consequence of the SNeIa sample having the largest weight in the chi-square minimization because of the highest number of data points with respect to other data sets;
- with three cosmographic parameters the differences between using total and cut samples decrease. Best

results always come from the cut samples but this time, differently from the previous point, they are related to the high-redshift extended priors, while assuming priors in the series convergence radius range does not satisfy the MCMC convergence requirements. This is somewhat expected from discussion in § (III), and possibly due to the fact that adding a third parameter in the restricted redshift range does not give any further improvement, while needing it for comparing cosmographic series with larger redshift ranges;

- adding GRBs to SNeIa (it was interesting to verify what happens when joining these data sets because they constitute an homogeneous sample as they are both based on the definition of the distance modulus) when considering two cosmographic parameters does not improve the analysis resulting in a very high chi-square value. When working with three cosmographic parameters the only statistically good results come from the cut samples. But in these cases the weight of GRBs is low (only 19 GRBs have redshift less than one) and no statistically significant changes are detected in the estimation of cosmographic parameters;
- the contribution of BAO data is almost statistically insignificant;
- adding only Hubble data to SNeIa in the two parameters case, while considering the total sample case, slightly increases chi-square value and produces different values for cosmographic parameters. Introducing the prior on positiveness of physical quantities on the Hubble data redshift range makes cosmographic estimations more similar to the SNeIa-only case. On the other side, when working with three parameters we detect an higher influence of Hubble data in the chi-square balance, with even largest (and previously undetected) deviations when applying the prior on positiveness $z < 1.76$. A further discussion on the reconstructed cosmological scenario is given in § (VI).

With these considerations in mind, we can take a look to the cosmographic parameters coming from using only SNeIa and considering just two parameters: the deceleration and the jerk. This is the most popular cosmographic parametrization in the literature so that our results and the advantages of the MCMC method can be easily judged and tested. We also underline that all the results in the literature are taken from sample of SNeIa where no redshift cut is applied.

As we have pointed before, there is a dependence of results from priors and from using cut or total sample which gets clear when looking to Fig. (5). If we move from the total sample and the prior applied on the total redshift range $z > 0$ (top panel), to the total sample with prior applied on the SNeIa redshift range (middle panel), and finally to the cut sample with prior in the z -redshift

convergence series radius, we detect a trend in the cosmographic parameters: the deceleration starts far from usual values in literature (and Λ CDM one too) and moves towards them, while jerk starts from a value very near to the Λ CDM one and which agrees perfectly with most of the results in literature, and moves to smaller values.

Considering the best chi-square values of the deceleration parameter, we remember that we are just using the Union2 data set from [30], which mixes many independent SNeIa observations so we may expect some differences with results like the ones in [1]. It is also interesting to underline that we agree with the analysis from [38], which uses a completely physically different data set, the X-ray observations of galaxy clusters, together with Gold and Legacy supernovae. Their method is also different: while in [1] they use the same series expansion approach as we do, in [38] an alternative numerical way leading to analytically exact functions was defined. The main difference in our work with respect to [1] is the use of physical constrains. Giving our agreement with the exact analytical approach from [38], we may argue that these constrains are an irrefutable requirement when working with cosmography as a series expansion tool. Finally, we perfectly agree at 1σ confidence level with the results in [5], while only slightly agree with results in [10] coming from the application of cosmography to high redshifts using gamma ray burst data.

About the jerk parameter it can be verified there is a good agreement with the analysis from X-ray emission from clusters of galaxies described in [38] and with the value coming from the Gold data set in [1], just as in the deceleration case.

At the same time we underline that it is also nude-eye visible that the error bars coming out from our analysis are actually narrower than in any other case (except for [5], who derives cosmographic parameters from theoretical assumptions without using any observational data). If we consider that we are working with a physically homogeneous sample (it is made of SNeIa only) but built from different (observationally and technically reduced) data sets, this positive result may be strongly related to the chosen statistical method, thus MCMC are showing their good nature with respect to other popular fitting procedures.

When moving to the three dimensional analysis, including the possibility of constraining the snap parameter, we find very different results. If we consider only the SNeIa sample, now the deceleration parameter is less negative and the jerk even changes sign becoming negative. We find a very weak match with past values from literature mainly due to their large errors. On the contrary, using MCMC makes us able to narrow down the confidence levels strongly.

The discussion cannot be complete without considering the value of the snap. Unfortunately we have not many examples in the literature we can compare with: from [39] and [10] we have some strongly positive values with percentage errors much larger than the 200%, while our anal-

ysis gives a negative value with narrower constraints. We remind the reader that the snap value in Λ CDM should be equal to -0.35 ; in this sense, the sign we have found shows a clear trend in this parameter and in the cosmological properties subtended by it.

When adding Hubble data, we have two different situations related to the different applied priors: when the positiveness is for $z > 0$ we find the main differences for the jerk, which is much more negative, and for the snap, less negative; on the other side, when the positiveness is for $z < 1.76$, differences are more pronounced: the deceleration is very near to -1 , while the jerk and the snap are positive and larger than before, 3.134 and 4.399 respectively. It is not an easy task to understand why this happens; moreover no correspondence with past values in literature is found.

C. y -redshift

If we work with the y -redshift defined in [1] to solve the convergence problem of the series, looking at Tables (III) - (IV) we can find some interesting changes:

- as expected from the definition of the y -redshift, differences both among total and cut samples and using different y -redshift prior ranges are strongly softened because we are always well inside the convergence radius of the series;
- results are always consistent and uniform, showing only small statistical variations, when considering two and three cosmographic parameters separately, but cosmographic estimations are different between the two and the three dimensional approach;
- adding high order y -redshift data (GRBs) to SNeIa does not change results in a significant statistical way. We have to remind that the y -redshift series show problem in reconstructing the distance modulus for $y \approx 0.4 \div 0.5$, which is well under the SNeIa maximum redshift even. So, we feel that this feature mostly depends on the intrinsic impossibility of y -redshift series to match the analytically exact physical behavior of distance modulus;
- BAO has no weight on the estimation of cosmographic parameters;
- as happened in the z -redshift case, here too Hubble data are the only exception in the uniformity of results exhibiting a stronger weight in the cosmographic estimations with respect of GRBs and BAO. While the contribution of the cut Hubble sample is not significant, the total one, extended up to $z = 1.76$, i.e. $y = 0.638$, produces the largest deviation. As the Hubble sample does not extend the y -redshift range in a much sensible way for explaining such a deviation, we can only argue that some peculiarities in Hubble high redshift data

are present also inducing the difficulties in fitting them as discussed in § (VI). A corroborating test for this explanation is the not reached convergence for MCMC in the three dimensional analysis when the total Hubble data sample is considered.

When comparing our results with the literature, the only previous examples where the y -redshift was used can be found in [1]. As in our case, when moving from z -redshift to y -redshift they found an increase in errors (which are bigger than ours, anyhow) of the cosmographic parameters, more consistent in the case of the jerk, as we have verified. This could be given by the substantial down-stretching of the redshift data when using this different parametrization; even if the physical content of the data is not altered, it is more difficult to extract cosmographic results when the data are flattened on the new redshift axes. The z -redshift range of the Union2 data set, $0 < z < 1.4$, goes over to the y -redshift interval $0 < y < 0.584$; Hubble data convert from $0 < z < 1.76$ to $0 < y < 0.638$, and GRBs from $0 < z < 6.6$ to $0 < y < 0.871$. It is clear that if we consider the great contribution from SNeIa to the chi-square function, we are fitting our physical distances on a limited range (low y -redshift) with respect to the total convergence radius ($y = 1$) so that higher order parameters (as the jerk and the snap) can be not as well estimated as lower order ones. Thus while for the deceleration parameter errors still remain quite centrally based, for the jerk case we have a long tail for high positive values (nearer the Λ CDM value but only matching it at 2σ confidence level) while for the snap we have a tail for large negative values matching the corresponding Λ CDM value. This may be considered a trend which one eventually needs to test and confirm if having higher order data.

The agreement is good for most of the past works we have considered, with the greatest number of successful matchings for the deceleration parameter than for the jerk. Anyway, the best results at all, come from the case where we use the full data samples and applied the prior in the range depicted by them. In this case also the deceleration and the jerk match well with the corresponding Λ CDM values.

VI. EQUIVALENT CPL MODEL

To round up results from simulations on cosmographic parameters, we can go deeper into the analysis and try to our results with a specific cosmological model. It is easy to check the link between them. In this paper we have used the CPL parametrization for dark energy given by Eq. (17) which depends only on three parameters, (Ω_m , w_0 and w_a). Using Eqs. (19) - (20) - (21) we can relate cosmographic parameters and CPL ones. We have different possibilities depending on the number of cosmographic parameters we are working with and on how many CPL parameters we are going to consider as free. In the end we have:

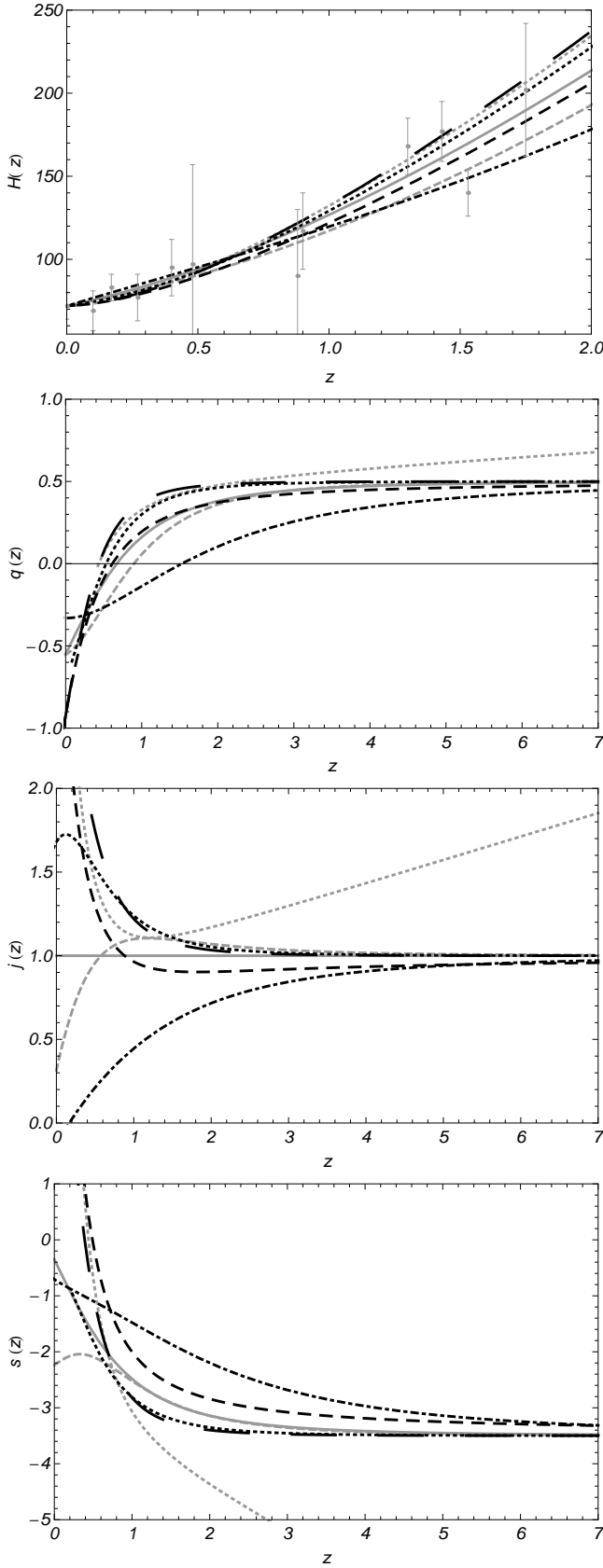


Figure 4. Hubble parameter $H(z)$ and cosmographic parameters $q(z)$, $j(z)$, $s(z)$ in different cosmological scenarios: Λ CDM model (solid gray line); Komatsu et al. (2010) model (dashed gray line); Perivolaropoulos et al. (2008) model (dotted gray line); Model I (long-dashed black line); Model II (short-dashed black line); Model III (dot-dashed black line); Model IV (dotted black line).

- with two cosmographic parameters, (q_0, j_0) , we can derive news about a Constant Dark Energy (CDE) model (i.e. $w_a = 0$), with:

$$\begin{aligned}\Omega_m(q_0, j_0) &= \frac{2(j_0 - q_0 - 2q_0^2)}{1 + 2j_0 - 6q_0}, \\ w_0(q_0, j_0) &= \frac{1 + 2j_0 - 6q_0}{-3 + 6q_0};\end{aligned}\quad (38)$$

- with two cosmographic parameters, (q_0, j_0) , we can derive news also about a Dynamical Dark Energy (DDE) model, (i.e. $w_a \neq 0$), leaving Ω_m free, with:

$$\begin{aligned}w_0(q_0, j_0, \Omega_m) &= \frac{1 - 2q_0}{3(-1 + \Omega_m)}, \\ w_a(q_0, j_0, \Omega_m) &= \frac{1}{3(-1 + \Omega_m)^2} (-2j_0(-1 + \Omega_m) - 2q_0 \\ &\quad \times (1 + 2q_0) + \Omega_m(-1 + 6q_0));\end{aligned}\quad (39)$$

- with three cosmographic parameters, (q_0, j_0, s_0) , we can derive news about a Dynamical Dark Energy (DDE) model, with Ω_m depending on cosmographic parameters, i.e. $\Omega_m \doteq \Omega_m(q_0, j_0, s_0)$. The same holds true for $w_0 \doteq w_0(q_0, j_0, s_0)$ and $w_a \doteq w_a(q_0, j_0, s_0)$. These expressions are much longer than previous ones and we do not write them here for the sake of brevity.

The most important thing is that with these relations all the statistical properties of these parameters (median, error bars, etc.) can be easily extracted from the cosmographic samples we have obtained from MCMC simulations. Final results of this dark energy analysis are reported in the tables on previous pages.

The first main result concerns Hubble data and their relation with the CDE model available from using cosmographic series with two parameters: when using z -redshift, this dynamical model is always unable to fit Hubble data. Even if we consider the model with parameters directly obtained from using this kind of data, we are only able to fit few points at very low redshift and not all the sample. Moreover, when moving to the CDE models with y -redshift and to the DDE models derived from three cosmographic parameters using Hubble data, we can easily verify that the derived cosmological parameters (and the cosmographic one too, as we pointed out in §. (V)) are always very different from the ones derived from other kinds of observational data. This feature can be interpreted in two different ways:

- it depends on the procedure which Hubble data are obtained from;
- there is an intrinsic information about the dynamical model in Hubble data.

Surely, for the two cosmographic parameters case, a better way of proceeding may be to obtain Ω_m from alternative ways and then join results with those one from cosmography as we discuss later in this section.

If we consider the CDE model derived from two cosmographic parameters and the DDE models derived from three cosmographic parameters with y -redshift, we can see that:

- Ω_m is lower than usual, being ≈ 0.07 , and matching at the top 1σ confidence level the usual estimation of $\Omega_m \sim 0.16$ obtained considering plasma contribution;
- if we also add Hubble data, then the value for the matter content grows up to ≈ 0.40 in the CDE case and to ≈ 0.36 in the DDE case. In both cases the bottom 1σ confidence limit matches the matter content value (plasma included) and the total Λ CDM one.

It is much intriguing to find such small values. Generally from SNeIa one is able to extract a slightly overestimated value of $\Omega_m \sim 0.30$ in [40]; in [15], unifying SNeIa, BAO and WMAP7, a value for $\Omega_m \sim 0.245$ was obtained; while in [38] it is $\Omega_m = 0.306^{+0.042}_{-0.040}$. We underline that any conclusion about the real possibility of such universe dynamics is out of the purpose of this paper. We have to consider that we are always working with an approximated approach (series expansion) and that this conclusion should be corroborated by a more extended analysis of all the other dynamical aspects of universe (formation of any gravitational structure, explanation of acceleration of universe). Then we need to refine the use and the approach of cosmography (what we are intended to do with a series of papers).

In the same cases as before, for what concerns the dark energy parameters, we have:

- for the CDE models, $w_0 \approx -0.82$, excluding the phantom line crossing at 1σ level; while adding Hubble data it becomes much more negative, $w_0 \approx -1.59$;
- for the DDE models, $w_0 \approx -0.715$ and $w_a \approx 0.01$ (~ -0.16 at 1σ error); adding Hubble data we get $w_0 \approx -1.272$ and $w_a \approx -0.326$.

The DDE models from two cosmographic parameters have Ω_m fixed at the value obtained in [15], while the dark energy parameters are:

- with the z -redshift, $w_0 \approx -1$ and $w_a \approx -0.71$; adding Hubble data they change to $w_0 \approx -1.4$ and $w_a \approx -1.2$, but they also have high chi-square values. About the w_a parameter, the question is very subtle and tricky: we have a negative value for it very far from the usual theoretical expected values and almost of the same order of w_0 .
- with the y -redshift, $w_0 \approx -1$ and $w_a \approx -0.56$ which match well the results from [15], $w_0 = -0.93$ and $w_a = -0.41$. Adding Hubble data they change to $w_0 \approx -1.25$ and $w_a \approx 1.2$. In this case, on the contrary, the value of w_a is of the same order of w_0

but positive so that $w_0 + w_a \sim 0$ and agrees with results from [41] where starting from Union SNeIa sample find $w_0 = -1.4$ and $w_a = 2$.

To test all this results we can also verify that considering the evolution of Hubble parameter or of the deceleration parameter, we do not find particular problems, but rather some intriguing properties. Using Eqs. (18) we can derive the functions $q(z, \Omega_m, w_0, w_a)$, $j(z, \Omega_m, w_0, w_a)$ and $s(z, \Omega_m, w_0, w_a)$. In this way, giving the cosmological model obtained by our cosmographic analysis and parameterized by the CPL prescription, we can infer the redshift dependence of the cosmographic parameters. In Fig. (4) we have plotted the analytical behavior of $H(z)$, $q(z)$, $j(z)$ and $s(z)$ for five different cosmological models:

- Λ CDM: $\Omega_m = 0.30$, $w_0 = -1$, $w_a = 0$;
- best cosmological model from [15]: $\Omega_m = 0.245$, $w_0 = -0.93$, $w_a = -0.41$;
- best cosmological model from [41]: $\Omega_m = 0.30$, $w_0 = -1.4$, $w_a = 2$;
- Model I, CDE model from two dimensional cosmographic analysis, in y -redshift applying priors only in the redshift range depicted by using all the data samples: $\Omega_m = 0.399$, $w_0 = -1.581$;
- Model II, DDE model from two dimensional cosmographic analysis, in y -redshift applying priors only in the redshift range depicted by using all the data samples: $\Omega_m = 0.245$, $w_0 = -1.256$, $w_a = 1.220$;
- Model III, DDE model from three dimensional cosmographic analysis, in z -redshift applying priors in the full z -redshift range and using all the data samples: $\Omega_m = 0.151$, $w_0 = -0.652$, $w_a = -0.207$;
- Model IV, DDE model from three dimensional cosmographic analysis, in y -redshift applying priors only in the redshift range depicted by using all the data samples: $\Omega_m = 0.364$, $w_0 = -1.272$, $w_a = -0.326$;

The first thing we can say is that our models can be different from the Λ CDM scenario for low redshifts, but they are equivalent to it for high redshifts. This is not the case of the model in [41], which is completely different from Λ CDM model at any redshift. Of course, in our case, we have the pleasant property of that some properties at high redshift (such as CMB theory and data) remain untouched; but, of course, the necessity of re-discussing what happens at low redshifts cannot be waived.

Considering Model I, for example, it has a transition from positive to negative $q(z)$ at $z = 0.44$ while this happens at $z = 0.68$ in a Λ CDM scenario. At the same time, transition from a matter dominated epoch to a dark energy dominated one happens at $z \sim 0.1$ in our model, while it is at $z = 0.32$ in Λ CDM.

Considering Model II, for example, it has a transition from positive to negative $q(z)$ at $z = 0.62$ and from dark matter to dark energy domination at $z \sim 0.42$. Even if it has dynamical parameters different from the Λ CDM ones, it also exhibits gross properties that are very similar to the consensus model, but at the same time the jerk and the snap behavior are much different only converging to Λ CDM values at high redshifts.

Model III and IV are different from previous models because dark energy fluid (given our CPL parameters values) has always been an *important* ingredient of universe dynamics with negative pressure (w_a is negative). The Model III seems to be the most problematic showing a transition from positive to negative $q(z)$ at $z = 1.52$ and from dark matter to dark energy domination at $z \sim 1.23$. On the contrary, Model IV shows more normal properties, as a transition from positive to negative $q(z)$ at $z = 0.53$ and from dark matter to dark energy domination at $z \sim 0.16$ also exhibiting very similar trends for the jerk and the snap.

VII. CONCLUSIONS

In this paper we are intended to perform a very detailed analysis of Cosmography, to state its degree of usability and extendibility when used as a model to universe dynamics.

First of all we have shown that results from a cosmographic approach are *sub-judice* because of the observational errors of cosmological data one works with. When working with cosmography one has to choose the highest order of expansion for the series of the $a(t)$ function so stating how many cosmographic (i.e. cosmological) parameters it is possible to extract from the analysis. But we have seen that differences between using a two, three or four dimensional series are well inside the errors given by data, so that (at the moment) any possibility of exactly stating what kind of series is better to be used is out of question.

From statistical considerations, we have seen that working with the series expansion approach, it is possible to derive up to a maximum of three cosmographic parameters, the deceleration, the jerk and the snap. Finally, the statistical method we have chosen to work with,

MCMC, gives us the possibility to sensibly narrow down the confidence errors on cosmographic parameters with respect to other results in the literature (coming from the same series approach).

Then MCMCs give also the possibility to manage priors on physical quantities. Comparing results with the literature we see that inside the narrower errors our estimations still agree with many works; what is more interesting, is that they also agree with a different approach leading to numerical evaluation of an exact analytical function of distance modulus ([38]).

What is even more interesting is what seems to come out from the analysis of dark energy parameters (in the CPL parametrization) related to the set of cosmographic parameters we have found out. We also know that Cosmography could be used as an independent tool to detect possible deviations from the Λ CDM model; but until now nobody has checked what the obtained cosmographic sets means in terms of dynamical information.

We have tried to give an answer, but this is still quite puzzling: cosmographic sets can be related to DE models which are quite slightly different from Λ CDM (at least at low redshifts). At the same time, smaller differences in the Cosmographic parameters values can give great differences in the dynamical cosmological model. For example we have seen that in the case of two cosmographic parameters, when working with only SN, we have a good agreement with literature. But these values correspond to a constant dark energy model with a low matter content. At the same time, this model is not able to fit Hubble data at high redshift.

Finally, very different global dynamics properties, can produce the same gross trends for Hubble and deceleration parameters (as much the jerk and the snap ones) pose the question of a possible cosmological dynamical degeneracy in the universe, which also makes more difficult to eventually detect alternative scenarios to Λ CDM.

In this optics developing cosmography is most important giving the possibility to discriminate among models using absolute values of cosmographic parameters. We think that all these questions could be solved improving the series expansion approach of Cosmography: we are studying the possibility to define an *Exact Cosmography* which could be solve the cosmographic degeneracy. A detailed description of this approach will be given in a forthcoming paper.

-
- [1] Cattoën, C., Visser, M., 2007, *Class. Quant. Grav.*, 24, 5985
 - [2] Cattoën, C., Visser, M., 2007, arXiv:gr-qc/0703122
 - [3] Visser, M., 2004, *Class. Quant. Grav.*, 21, 2603
 - [4] John, M. V., 2005, *ApJ*, 630, 667
 - [5] Poplawski, N. J., 2006, *Phys. Lett. B*, 640, 135
 - [6] Poplawski, N. J., 2007, *Class. Quant. Grav.*, 24, 3013
 - [7] Capozziello S., Cardone V.F., Salzano V., 2008, *Phys. Rev. D* 78, 063504.
 - [8] Bouhmadi-Lopez, M., Capozziello S., Cardone V.F., 2010, *Phys.Rev.D* 82, 103526.
 - [9] Balcerzak A., Dabrowski M. P., 2010, *Phys. Rev. D* 81, 123527.
 - [10] Capozziello, S., Izzo, L., 2008, *A&A*, 490, 31
 - [11] Izzo L., Capozziello S., Covone G., Capaccioli M., 2009, *Astron. Astroph.* 508, 63 (2009).
 - [12] Dunajski, M., Gibbons, G., 2008, *Class. Quant. Grav.*, 25, 235012

- [13] Chevallier, M., Polarski, D., *Int. J. Mod. Phys. D.*, 2001, 10, 213
- [14] Linder, E.V., *Phys. Rev. Lett.*, 2003, 90, 091301
- [15] Komatsu, E., et al., submitted to *ApJS*, arXiv:1001.4538
- [16] Stern, D., Jimenez, R., Verde, L., Kamionkowski, M., Stanford, A., 2010, *JCAP*, 1, 2, 8
- [17] Simon, J., Verde, L., Jimenez, R., 2005, *Phys. Rev. D*, 71, 123001
- [18] Mörtzell, E., Jöhnsson, J., arXiv:1102.4485
- [19] Jimenez, R., Loeb, A., 2002, *ApJ*, 573, 37
- [20] Jimenez, R., Verde, L., Treu, T., Stern, D., 2003, *ApJ*, 593, 622
- [21] Stern, D., Jimenez, R., Verde, L., Stanford, A., Kamionkowski, M., 2010, *ApJS*, 188, 280-289
- [22] Stern, D., 2000, arXiv:astro-ph/0012146
- [23] Le Fèvre, O., et al., 2005, *A&A*, 439, 845
- [24] Jimenez, R., MacDonald, J., Dunlop, J.S., Padoan, P., Peacock, J.A., 2004, *MNRAS*, 349, 240
- [25] Riess, Adam G. and others, 2009, *ApJ*, 699, 539-563
- [26] Berg, B.A., *Markov Chain Monte Carlo Simulations and Their Statistical Analysis*, World Scientific Publishing Co. Pte. Ltd., Singapore
- [27] MacKay, D. J. C., 2003, *Information Theory, Inference, and Learning Algorithms*, Cambridge University Press
- [28] Neal, R.M., *25 September 1993, Technical Report CRG-TR-93-1*, Department of Computer Science, University of Toronto
- [29] Dunkley, J., Bucher, M., Ferreira, P. G., Moodley, K., Skordis K., 2005, *MNRAS*, 356, 925
- [30] Amanullah, R., et al., 2010, *ApJ*, 716, 712-738
- [31] Kowalski, M., Rubin, D., Aldering, G. et al., 2008, *ApJ*, 686, 749
- [32] Amanullah, R., et al., 2008, *A&A*, 486, 375
- [33] Hicken, M., et al., 2009a, *ApJ*, 700, 331-357
- [34] Holtzman, J.A., et al., 2008, *AJ*, 136, 2306
- [35] Cardone, V. F., Capozziello, S., Dainotti, M.G., 2009, *MNRAS*, 440, 775
- [36] Schaefer, B.E., 2007, *ApJ*, 660, 16
- [37] Percival, W.J., et al., 2010, *MNRAS*, 401, 2148
- [38] Rapetti, D., Allen, S.W., Amin, A., Blandford, R.D., 2007, *MNRAS*, 375, 1510
- [39] John, M. V., 2004, *ApJ*, 614, 1
- [40] Bueno Sanchez, J.C., Nesseris, S., Perivolaropoulos, L., 2009, *JCAP*, 11, 29
- [41] Perivolaropoulos, L., Shafieloo, A., 2009, *Phys. Rev. D*, 79, 123502
- [42] Vitagliano, V., Xia J.-Q., Liberati, S., Viel, M., 2010, *JCAP*, 03, 005

Appendix A: Cosmological distances in Cosmography

The physical distance traveled by a photon emitted at time t_* and absorbed at the current epoch t_0 is

$$D = c \int dt = c(t_0 - t_*), \quad (\text{A1})$$

so that inserting $t_* = t_0 - D/c$ into Eq. (3) gives us an expression for the redshift as a function of t_0 and D/c , i.e. $z = z(D)$. Solving with respect to D , up to the fifth

order in z , gives us the desired expansion for $D(z)$:

$$D(z) = \frac{cz}{H_0} \left\{ \mathcal{D}_z^0 + \mathcal{D}_z^1 z + \mathcal{D}_z^2 z^2 + \mathcal{D}_z^3 z^3 + \mathcal{D}_z^4 z^4 + O[z^5] \right\}. \quad (\text{A2})$$

In the latter we have defined

$$\begin{aligned} \mathcal{D}_z^0 &= 1, \\ \mathcal{D}_z^1 &= - \left(1 + \frac{q_0}{2} \right), \\ \mathcal{D}_z^2 &= 1 + q_0 + \frac{q_0^2}{2} - \frac{j_0}{6}, \\ \mathcal{D}_z^3 &= - \left(1 + \frac{3}{2}q_0 + \frac{3}{2}q_0^2 + \frac{5}{8}q_0^3 - \frac{1}{2}j_0 - \frac{5}{12}q_0j_0 - \frac{s_0}{24} \right), \\ \mathcal{D}_z^4 &= 1 + 2q_0 + 3q_0^2 + \frac{5}{2}q_0^3 + \frac{7}{2}q_0^4 - \frac{5}{3}q_0j_0 - \frac{7}{8}q_0^2j_0 \\ &\quad - j_0 + \frac{j_0^2}{12} - \frac{1}{8}q_0s_0 - \frac{s_0}{6} - \frac{l_0}{120}. \end{aligned}$$

The Taylor series expansion of the quantity $D(z)$ is a building block for other quantities to be derived in the following sections as required by the cosmographic approach.

In typical applications, one is not interested in the physical distance $D(z)$, but in other definitions. In our case, the *luminosity distance*,

$$D_L = \frac{a(t_0)}{a(t_0 - D/c)} (a(t_0)r_0(D)), \quad (\text{A3})$$

has a particular relevance. In Eq. (A3) we have used

$$r_0(D) = \begin{cases} \sin \int_{t_0 - D/c}^{t_0} \frac{cdt}{a(t)} & k = 1, \\ \int_{t_0 - D/c}^{t_0} \frac{cdt}{a(t)} & k = 0, \\ \sinh \int_{t_0 - D/c}^{t_0} \frac{cdt}{a(t)} & k = -1. \end{cases} \quad (\text{A4})$$

Using Eq. (A2), and after some lengthy algebra, we obtain

$$\begin{aligned} \frac{r_0(D)}{D/a_0} &= \mathcal{R}_D^0 + \mathcal{R}_D^1 \left(\frac{H_0 D}{c} \right) + \mathcal{R}_D^2 \left(\frac{H_0 D}{c} \right)^2 \\ &\quad + \mathcal{R}_D^3 \left(\frac{H_0 D}{c} \right)^3 + \mathcal{R}_D^4 \left(\frac{H_0 D}{c} \right)^4 + \mathcal{R}_D^5 \left(\frac{H_0 D}{c} \right)^5, \end{aligned}$$

with

$$\begin{aligned} \mathcal{R}_D^0 &= 1, \\ \mathcal{R}_D^1 &= \frac{1}{2}, \\ \mathcal{R}_D^2 &= \frac{1}{6} \left[2 + q_0 - \frac{kc^2}{H_0^2 a_0^2} \right], \\ \mathcal{R}_D^3 &= \frac{1}{24} \left[6 + 6q_0 + j_0 - 6 \frac{kc^2}{H_0^2 a_0^2} \right], \end{aligned}$$

$$\begin{aligned}\mathcal{R}_D^4 &= \frac{1}{120} \left[24 + 36q_0 + 6q_0^2 + 8j_0 - s_0 - \frac{5kc^2(7+2q_0)}{a_0^2 H_0^2} \right], \\ \mathcal{R}_D^5 &= \frac{1}{120} \left[24 + 48q_0 + 18q_0^2 + 4q_0 j_0 + 12j_0 - 2s_0 + 24l_0 \right. \\ &\quad \left. - \frac{3kc^2(15+10q_0+j_0)}{a_0^2 H_0^2} \right].\end{aligned}$$

$$\begin{aligned}\mathcal{D}_L^3 &= \frac{1}{24} [50 - 26q_0 + 21q_0^2 - 15q_0^3 - 7j_0 + 10q_0 j_0 + s_0], \\ \mathcal{D}_L^4 &= \frac{1}{120} [274 - 154q_0 + 141q_0^2 - 135q_0^3 + 105q_0^4 + 10j_0^2 \\ &\quad - 47j_0 + 90q_0 j_0 - 105q_0^2 j_0 - 15q_0 s_0 + 9s_0 - l_0].\end{aligned}\tag{B2}$$

One now must rewrite $r_0(D)$ as a function of z using Eq. (A2). Inserting the result into Eq. (A3), one obtains the fifth order approximation for the Hubble free luminosity distance $d_L = D_L(z)/(c/H_0)$ as a function of the redshift z :

$$d_L(z) = \mathcal{D}_L^0 z + \mathcal{D}_L^1 z^2 + \mathcal{D}_L^2 z^3 + \mathcal{D}_L^3 z^4 + \mathcal{D}_L^4 z^5. \tag{A5}$$

In the latter we are using the definitions

$$\begin{aligned}\mathcal{D}_L^0 &= 1, \\ \mathcal{D}_L^1 &= -\frac{1}{2} [-1 + q_0], \\ \mathcal{D}_L^2 &= -\frac{1}{6} \left[1 - q_0 - 3q_0^2 + j_0 + \frac{kc^2}{H_0^2 a_0^2} \right], \\ \mathcal{D}_L^3 &= \frac{1}{24} [2 - 2q_0 - 15q_0^2 - 15q_0^3 + 5j_0 + 10q_0 j_0 + s_0 \\ &\quad + \frac{2kc^2(1+3q_0)}{H_0^2 a_0^2}], \\ \mathcal{D}_L^4 &= \frac{1}{120} [-6 + 6q_0 + 81q_0^2 + 165q_0^3 + 105q_0^4 + 10j_0^2 \\ &\quad - 27j_0 - 110q_0 j_0 - 105q_0^2 j_0 - 15q_0 s_0 - 11s_0 - l_0 \\ &\quad - \frac{5kc^2(1+8q_0+9q_0^2-2j_0)}{a_0^2 H_0^2}].\end{aligned}\tag{A6}$$

Previous relations in this section have been derived for any value of the curvature parameter; in [42], it is shown that ranging the curvature parameter in the interval $[-1, 1]$ has negligible effects on the estimation of cosmographic parameters, so that, in the following of the paper, we will assume a flat universe and use the simplified versions with $k = 0$.

Appendix B: Y redshift relations

We write here all the needed relations expressed in term of the y-redshift for $k = 0$. The Hubble free luminosity distance $d_L(y)$ is:

$$d_L(y) = \mathcal{D}_L^0 y + \mathcal{D}_L^1 y^2 + \mathcal{D}_L^2 y^3 + \mathcal{D}_L^3 y^4 + \mathcal{D}_L^4 y^5, \tag{B1}$$

where

$$\begin{aligned}\mathcal{D}_L^0 &= 1, \\ \mathcal{D}_L^1 &= \frac{3}{2} [1 - q_0], \\ \mathcal{D}_L^2 &= \frac{1}{6} [11 - 5q_0 + 3q_0^2 - j_0],\end{aligned}$$

The distance modulus is

$$\mu(y) = \frac{5}{\log 10} \cdot (\log y + \mathcal{M}^1 y + \mathcal{M}^2 y^2 + \mathcal{M}^3 y^3 + \mathcal{M}^4 y^4), \tag{B3}$$

with

$$\begin{aligned}\mathcal{M}^1 &= \frac{3}{2} [1 - q_0], \\ \mathcal{M}^2 &= \frac{1}{24} [17 - 2q_0 + 9q_0^2 - 4j_0], \\ \mathcal{M}^3 &= \frac{1}{24} [11 - q_0 + 2q_0^2 - 10q_0^3 - j_0 + 8q_0 j_0 + s_0], \\ \mathcal{M}^4 &= \frac{1}{2880} [971 - 76q_0 + 134q_0^2 - 300q_0^3 + 1575q_0^4 + 200j_0^2 \\ &\quad - 68j_0 + 260q_0 j_0 - 1800q_0^2 j_0 - 300q_0 s_0 + 36s_0 \\ &\quad - 24l_0].\end{aligned}\tag{B4}$$

The Hubble parameter is

$$\begin{aligned}H(y) &= H_0 \cdot (\mathcal{H}_0^0 + \mathcal{H}_0^1 y + \mathcal{H}_0^2 y^2 + \mathcal{H}_0^3 y^3 \\ &\quad + \mathcal{H}_0^4 y^4)\end{aligned}\tag{B5}$$

where

$$\mathcal{H}_0^0 = 1, \tag{B6}$$

$$\mathcal{H}_0^1 = 1 + q_0, \tag{B7}$$

$$\mathcal{H}_0^2 = 1 + \frac{j_0}{2} + q_0 - \frac{q_0^2}{2}, \tag{B8}$$

$$\mathcal{H}_0^3 = \frac{1}{6} [6 + 6q_0 - 3q_0^2 + 3q_0^3 + 3j_0 - 4j_0 q_0 - s_0] \tag{B9}$$

$$\begin{aligned}\mathcal{H}_0^4 &= \frac{1}{24} [24 + 24q_0 - 12q_0^2 + 12q_0^3 - 15q_0^4 + 12j_0 - 4j_0^2 \\ &\quad - 16j_0 q_0 + 25j_0 q_0^2 - 4s_0 + 7q_0 s_0 + l_0],\end{aligned}\tag{B10}$$

The square of the Hubble parameter is

$$\begin{aligned}H^2(y) &= H_0^2 \left(\mathcal{H}_0^{2,0} + \mathcal{H}_0^{2,1} y + \mathcal{H}_0^{2,2} y^2 + \mathcal{H}_0^{2,3} y^3 \right. \\ &\quad \left. + \mathcal{H}_0^{2,4} y^4 \right),\end{aligned}\tag{B11}$$

where

$$\mathcal{H}_0^{2,0} = 1, \tag{B12}$$

$$\mathcal{H}_0^{2,1} = 2[1 + q_0], \tag{B13}$$

$$\mathcal{H}_0^{2,2} = 3 + 4q_0 + j_0, \tag{B14}$$

$$\mathcal{H}_0^{2,3} = 4 + 6q_0 + 2j_0 - \frac{j_0 q_0}{3} - \frac{s_0}{3}, \quad (\text{B15})$$

$$\begin{aligned} \mathcal{H}_0^{2,4} = & \frac{1}{12} [60 + 96q_0 + 36j_0 - j_0^2 - 8j_0q_0 + 3j_0^2q_0 - 8s_0 \\ & + 3q_0s_0 + l_0]. \end{aligned} \quad (\text{B16})$$

Appendix C: H derivatives

Here we report convenient expressions for the conversion from higher order derivatives in time to higher order derivatives in redshift:

$$\begin{aligned} \frac{d^2}{dt^2} = & (1+z)H \left[H + (1+z)\frac{dH}{dz} \right] \frac{d}{dz} \\ & + (1+z)^2 H^2 \frac{d^2}{dz^2}, \end{aligned} \quad (\text{C1})$$

$$\begin{aligned} \frac{d^3}{dt^3} = & -(1+z)H \left\{ H^2 + (1+z)^2 \left(\frac{dH}{dz} \right)^2 + (1+z)H \right. \\ & \times \left[4\frac{dH}{dz} + (1+z)\frac{d^2H}{dz^2} \right] \left. \right\} \frac{d}{dz} - 3(1+z)^2 H^2 \\ & \times \left[H + (1+z)\frac{dH}{dz} \right] \frac{d^2}{dz^2} - (1+z)^3 H^3 \frac{d^3}{dz^3}, \end{aligned} \quad (\text{C2})$$

$$\frac{d^4}{dt^4} = (1+z)H \left[H^2 + 11(1+z)H^2 \frac{dH}{dz} + 11(1+z)H \right.$$

$$\begin{aligned} & \times \frac{dH}{dz} + (1+z)^3 \left(\frac{dH}{dz} \right)^3 + 7(1+z)^2 H \frac{d^2H}{dz^2} \\ & + 4(1+z)^3 H \frac{dH}{dz} \frac{d^2H}{dz^2} + (1+z)^3 H^2 \frac{d^3H}{dz^3} \left. \right] \frac{d}{dz} \\ & + (1+z)^2 H^2 \left[7H^2 + 22H \frac{dH}{dz} + 7(1+z)^2 \left(\frac{dH}{dz} \right)^2 \right. \\ & + 4H \frac{d^2H}{dz^2} \left. \right] \frac{d^2}{dz^2} + 6(1+z)^3 H^3 \left[H + (1+z)\frac{dH}{dz} \right] \\ & \times \frac{d^3}{dz^3} + (1+z)^4 H^4 \frac{d^4}{dz^4} + (1+z)^4 H^4 \frac{d^4}{dz^4}. \end{aligned} \quad (\text{C3})$$

Appendix D: Square Hubble parameter

The expansion series of the square Hubble parameter, H^2 , will be a useful tool as well. It is a simple and just a long matter of algebra to compute its derivatives with the same procedure as above. The final results are

$$\frac{d(H^2)}{dt} = \frac{2H^2}{1+z} (1+q) \quad (\text{D1})$$

$$\frac{d^2(H^2)}{dt^2} = \frac{2H^2}{(1+z)^2} (1+2q+j) \quad (\text{D2})$$

$$\frac{d^3(H^2)}{dt^3} = \frac{2H^2}{(1+z)^3} (-qj-s) \quad (\text{D3})$$

$$\frac{d^4(H^2)}{dt^4} = \frac{2H^2}{(1+z)^4} (4qj+3qs+3q^2j-j^2+4s+l) \quad (\text{D4})$$

Table I. Results in the two dimensional parameter space (q_0, j_0) and z-redshift. Column (1): simulation identification in the text with the used data (S = SNeIa, G = GRBs, H = Hubble, B = BAO; the index (c) refers to the redshift-cut sub-sample, with $z < 1$) and the applied priors (we indicate the redshift range where positiveness of quantities described in § (V A) is applied). Columns (2) - (3) - (4): best fit estimations of cosmographic parameters with 1σ confidence level. Column (5): chi square and reduced chi square values. Columns (6) - (7) - (8) - (9): best fit estimations of dark energy (CPL) parameters with 1σ confidence level for the constant dark energy model and the dynamical one with fixed Ω_m as described in § (VI).

Data	Best fit parameters			CDE		DDE ($\Omega_m = 0.245$)	
S	q_0	j_0	χ^2 ($\chi^2/d.o.f.$)	Ω_m	w_0	w_0	w_a
$z > 0$	$-1.014^{+0.008}_{-0.013}$	$1.060^{+0.063}_{-0.035}$	622.11 (1.123)	$0.004^{+0.005}_{-0.003}$	$-1.013^{+0.008}_{-0.014}$	$-1.337^{+0.007}_{-0.011}$	$-1.295^{+0.005}_{-0.011}$
$z < 1.4$	$-0.738^{+0.043}_{-0.043}$	$0.372^{+0.099}_{-0.085}$	573.95 (1.036)	$0.005^{+0.009}_{-0.004}$	$-0.831^{+0.029}_{-0.031}$	$-1.093^{+0.039}_{-0.038}$	$-0.858^{+0.059}_{-0.059}$
$z > 0^{(c)}$	$-1.017^{+0.010}_{-0.017}$	$1.072^{+0.082}_{-0.045}$	599.21 (1.122)	$0.005^{+0.006}_{-0.003}$	$-1.016^{+0.010}_{-0.017}$	$-1.339^{+0.009}_{-0.014}$	$-1.295^{+0.005}_{-0.011}$
$z < 1^{(c)}$	$-0.669^{+0.049}_{-0.052}$	$0.284^{+0.151}_{-0.100}$	529.97 (0.992)	$0.019^{+0.027}_{-0.014}$	$-0.796^{+0.038}_{-0.049}$	$-1.033^{+0.043}_{-0.046}$	$-0.723^{+0.063}_{-0.064}$
S-G	q_0	j_0	χ^2 ($\chi^2/d.o.f.$)	Ω_m	w_0	w_0	w_a
$z > 0$	$-1.004^{+0.003}_{-0.005}$	$1.016^{+0.016}_{-0.011}$	1166.07 (1.872)	$0.0004^{+0.0038}_{-0.0032}$	$-1.003^{+0.002}_{-0.003}$	$-1.328^{+0.003}_{-0.004}$	$-1.293^{+0.014}_{-0.023}$
$z < 6.7$	$-0.507^{+0.026}_{-0.031}$	$0.010^{+0.034}_{-0.025}$	1015.14 (1.629)	$0.001^{+0.002}_{-0.001}$	$-0.672^{+0.017}_{-0.020}$	$-0.889^{+0.023}_{-0.027}$	$-0.578^{+0.030}_{-0.036}$
$z > 0^{(c)}$	$-1.016^{+0.009}_{-0.017}$	$1.068^{+0.084}_{-0.042}$	602.03 (1.089)	$0.004^{+0.007}_{-0.003}$	$-1.015^{+0.009}_{-0.018}$	$-1.338^{+0.008}_{-0.015}$	$-1.295^{+0.005}_{-0.010}$
$z < 1^{(c)}$	$-0.673^{+0.045}_{-0.050}$	$0.292^{+0.149}_{-0.096}$	533.20 (0.964)	$0.020^{+0.027}_{-0.015}$	$-0.799^{+0.035}_{-0.049}$	$-1.036^{+0.040}_{-0.044}$	$-0.727^{+0.065}_{-0.062}$
S-H	q_0	j_0	χ^2 ($\chi^2/d.o.f.$)	Ω_m	w_0	w_0	w_a
$z > 0$	$-1.159^{+0.059}_{-0.048}$	$1.859^{+0.291}_{-0.337}$	717.88 (1.268)	$0.056^{+0.015}_{-0.019}$	$-1.170^{+0.063}_{-0.053}$	$-1.464^{+0.052}_{-0.042}$	$-1.283^{+0.010}_{-0.011}$
$z < 1.76$	$-0.636^{+0.052}_{-0.056}$	$0.219^{+0.152}_{-0.095}$	637.70 (1.127)	$0.017^{+0.023}_{-0.013}$	$-0.771^{+0.040}_{-0.052}$	$-1.003^{+0.046}_{-0.049}$	$-0.689^{+0.055}_{-0.055}$
$z > 0^{(c)}$	$-1.016^{+0.010}_{-0.016}$	$1.069^{+0.081}_{-0.041}$	606.06 (1.118)	$0.004^{+0.006}_{-0.003}$	$-1.015^{+0.009}_{-0.017}$	$-1.339^{+0.008}_{-0.014}$	$-1.295^{+0.005}_{-0.010}$
$z < 1^{(c)}$	$-0.667^{+0.048}_{-0.051}$	$0.288^{+0.151}_{-0.103}$	532.80 (0.983)	$0.022^{+0.028}_{-0.016}$	$-0.797^{+0.039}_{-0.049}$	$-1.031^{+0.042}_{-0.046}$	$-0.714^{+0.065}_{-0.062}$
S-G-H	q_0	j_0	χ^2 ($\chi^2/d.o.f.$)	Ω_m	w_0	w_0	w_a
$z > 0$	$-1.004^{+0.002}_{-0.004}$	$1.015^{+0.015}_{-0.009}$	1267.78 (1.996)	$0.0005^{+0.0008}_{-0.0004}$	$-1.003^{+0.002}_{-0.003}$	$-1.328^{+0.002}_{-0.004}$	$-1.293^{+0.003}_{-0.006}$
$z < 6.7$	$-0.476^{+0.010}_{-0.018}$	$-0.019^{+0.017}_{-0.011}$	1050.51 (1.654)	$0.001^{+0.002}_{-0.001}$	$-0.652^{+0.007}_{-0.012}$	$-0.862^{+0.009}_{-0.016}$	$-0.543^{+0.011}_{-0.020}$
$z > 0^{(c)}$	$-1.017^{+0.010}_{-0.017}$	$1.074^{+0.086}_{-0.046}$	609.44 (1.086)	$0.005^{+0.007}_{-0.004}$	$-1.016^{+0.010}_{-0.018}$	$-1.340^{+0.009}_{-0.014}$	$-1.295^{+0.005}_{-0.010}$
$z < 1^{(c)}$	$-0.667^{+0.050}_{-0.052}$	$0.285^{+0.162}_{-0.104}$	535.94 (0.955)	$0.021^{+0.030}_{-0.015}$	$-0.796^{+0.040}_{-0.052}$	$-1.031^{+0.044}_{-0.046}$	$-0.714^{+0.068}_{-0.064}$
S-G-H-B	q_0	j_0	χ^2 ($\chi^2/d.o.f.$)	Ω_m	w_0	w_0	w_a
$z > 0$	$-1.004^{+0.002}_{-0.003}$	$1.014^{+0.016}_{-0.008}$	1267.61 (1.993)	$0.0005^{+0.0008}_{-0.0004}$	$-1.003^{+0.002}_{-0.003}$	$-1.328^{+0.002}_{-0.003}$	$-1.293^{+0.003}_{-0.006}$
$z < 6.7$	$-0.477^{+0.010}_{-0.018}$	$-0.018^{+0.017}_{-0.011}$	1051.21 (1.653)	$0.001^{+0.002}_{-0.001}$	$-0.653^{+0.007}_{-0.012}$	$-0.863^{+0.009}_{-0.016}$	$-0.544^{+0.011}_{-0.020}$
$z > 0^{(c)}$	$-1.016^{+0.009}_{-0.016}$	$1.072^{+0.080}_{-0.043}$	609.08 (1.084)	$0.005^{+0.007}_{-0.003}$	$-1.016^{+0.009}_{-0.017}$	$-1.339^{+0.008}_{-0.014}$	$-1.294^{+0.004}_{-0.010}$
$z < 1^{(c)}$	$-0.667^{+0.049}_{-0.050}$	$0.282^{+0.153}_{-0.104}$	536.17 (0.954)	$0.020^{+0.028}_{-0.015}$	$-0.795^{+0.040}_{-0.050}$	$-1.030^{+0.044}_{-0.044}$	$-0.715^{+0.065}_{-0.063}$
S-H-B	q_0	j_0	χ^2 ($\chi^2/d.o.f.$)	Ω_m	w_0	w_0	w_a
$z > 0$	$-1.152^{+0.052}_{-0.050}$	$1.819^{+0.308}_{-0.294}$	718.55 (1.267)	$0.055^{+0.015}_{-0.017}$	$-1.165^{+0.057}_{-0.055}$	$-1.459^{+0.046}_{-0.045}$	$-1.283^{+0.009}_{-0.010}$
$z < 1.76$	$-0.637^{+0.050}_{-0.059}$	$0.223^{+0.163}_{-0.092}$	638.01 (1.125)	$0.018^{+0.023}_{-0.013}$	$-0.773^{+0.038}_{-0.054}$	$-1.004^{+0.044}_{-0.051}$	$-0.691^{+0.054}_{-0.056}$
$z > 0^{(c)}$	$-1.017^{+0.010}_{-0.017}$	$1.074^{+0.083}_{-0.045}$	606.23 (1.116)	$0.005^{+0.007}_{-0.004}$	$-1.016^{+0.010}_{-0.017}$	$-1.339^{+0.009}_{-0.014}$	$-1.295^{+0.005}_{-0.010}$
$z < 1^{(c)}$	$-0.669^{+0.048}_{-0.051}$	$0.288^{+0.152}_{-0.105}$	532.98 (0.981)	$0.021^{+0.028}_{-0.015}$	$-0.797^{+0.040}_{-0.048}$	$-1.032^{+0.042}_{-0.045}$	$-0.718^{+0.065}_{-0.063}$

Table II. Results in the three dimensional parameter space (q_0, j_0, s_0) and z-redshift. Void rows correspond to MCMC which do not pass the convergence test. Column (1): simulation identification in the text with the used data ($S = \text{SNeIa}$, $G = \text{GRBs}$, $H = \text{Hubble}$, $B = \text{BAO}$; the index (c) refers to the redshift-cut sub-sample, with $z < 1$) and the applied priors (we indicate the redshift range where positiveness of quantities described in § (VA) is applied). Columns (2) - (3) - (4): best fit estimations of cosmographic parameters with 1σ confidence level. Column (5): chi square and reduced chi square values. Columns (6) - (7) - (8): best fit estimations of dark energy (CPL) parameters with 1σ confidence level for the dynamical dark energy model as described in § (VI).

Data	Best fit parameters				DDE		
S	q_0	j_0	s_0	$\chi^2 (\chi^2/d.o.f.)$	Ω_m	w_0	w_a
$z > 0$	—	—	—	—	—	—	—
$z < 1.4$	—	—	—	—	—	—	—
$z > 0^{(c)}$	$-0.319^{+0.045}_{-0.044}$	$-0.062^{+0.128}_{-0.275}$	$-0.680^{+0.456}_{-0.429}$	541.76 (1.016)	$0.158^{+0.066}_{-0.074}$	$-0.650^{+0.078}_{-0.073}$	$-0.213^{+0.129}_{-0.093}$
$z < 1^{(c)}$	—	—	—	—	—	—	—
S-G	q_0	j_0	s_0	$\chi^2 (\chi^2/d.o.f.)$	Ω_m	w_0	w_a
$z > 0$	—	—	—	—	—	—	—
$z < 6.7$	—	—	—	—	—	—	—
$z > 0^{(c)}$	$-0.319^{+0.045}_{-0.046}$	$-0.052^{+0.129}_{-0.286}$	$-0.688^{+0.464}_{-0.440}$	545.36 (0.988)	$0.159^{+0.067}_{-0.075}$	$-0.653^{+0.080}_{-0.073}$	$-0.214^{+0.128}_{-0.090}$
$z < 1^{(c)}$	—	—	—	—	—	—	—
S-H	q_0	j_0	s_0	$\chi^2 (\chi^2/d.o.f.)$	Ω_m	w_0	w_a
$z > 0$	$-0.219^{+0.025}_{-0.025}$	$-0.536^{+0.051}_{-0.040}$	$-0.203^{+0.061}_{-0.114}$	587.99 (1.041)	$0.110^{+0.018}_{-0.017}$	$-0.537^{+0.012}_{-0.015}$	$-0.409^{+0.028}_{-0.015}$
$z < 1.76$	$-0.944^{+0.032}_{-0.039}$	$3.134^{+0.063}_{-0.088}$	$4.399^{+0.463}_{-0.556}$	614.23 (1.087)	$0.379^{+0.017}_{-0.019}$	$-1.553^{+0.010}_{-0.013}$	$-0.295^{+0.027}_{-0.034}$
$z > 0^{(c)}$	$-0.322^{+0.045}_{-0.045}$	$-0.071^{+0.124}_{-0.257}$	$-0.657^{+0.437}_{-0.434}$	543.97 (1.005)	$0.151^{+0.062}_{-0.071}$	$-0.648^{+0.075}_{-0.071}$	$-0.212^{+0.132}_{-0.089}$
$z < 1^{(c)}$	—	—	—	—	—	—	—
S-G-H	q_0	j_0	s_0	$\chi^2 (\chi^2/d.o.f.)$	Ω_m	w_0	w_a
$z > 0$	—	—	—	—	—	—	—
$z < 6.7$	—	—	—	—	—	—	—
$z > 0^{(c)}$	—	—	—	—	—	—	—
$z < 1^{(c)}$	—	—	—	—	—	—	—
S-G-H-B	q_0	j_0	s_0	$\chi^2 (\chi^2/d.o.f.)$	Ω_m	w_0	w_a
$z > 0$	$0.336^{+0.021}_{-0.018}$	$0.131^{+0.045}_{-0.039}$	$-0.066^{+0.027}_{-0.024}$	1031.03 (1.624)	$0.329^{+0.018}_{-0.034}$	$-0.163^{+0.028}_{-0.022}$	$-0.456^{+0.024}_{-0.015}$
$z < 6.7$	—	—	—	—	—	—	—
$z > 0^{(c)}$	$-0.328^{+0.046}_{-0.046}$	$-0.051^{+0.135}_{-0.292}$	$-0.662^{+0.437}_{-0.432}$	549.42 (0.979)	$0.151^{+0.066}_{-0.070}$	$-0.652^{+0.075}_{-0.075}$	$-0.207^{+0.140}_{-0.096}$
$z < 1^{(c)}$	—	—	—	—	—	—	—
S-H-B	q_0	j_0	s_0	$\chi^2 (\chi^2/d.o.f.)$	Ω_m	w_0	w_a
$z > 0$	$-0.221^{+0.027}_{-0.025}$	$-0.538^{+0.053}_{-0.040}$	$-0.202^{+0.059}_{-0.108}$	590.19 (1.043)	$0.109^{+0.019}_{-0.016}$	$-0.538^{+0.012}_{-0.015}$	$-0.409^{+0.028}_{-0.015}$
$z < 1.76$	$-0.958^{+0.033}_{-0.026}$	$3.138^{+0.053}_{-0.052}$	$4.442^{+0.373}_{-0.389}$	615.64 (1.088)	$0.373^{+0.018}_{-0.012}$	$-1.551^{+0.010}_{-0.011}$	$-0.292^{+0.026}_{-0.030}$
$z > 0^{(c)}$	$-0.328^{+0.045}_{-0.045}$	$-0.063^{+0.138}_{-0.279}$	$-0.690^{+0.413}_{-0.452}$	545.50 (1.006)	$0.154^{+0.063}_{-0.073}$	$-0.654^{+0.077}_{-0.072}$	$-0.218^{+0.134}_{-0.089}$
$z < 1^{(c)}$	—	—	—	—	—	—	—

Table III. Results in the two dimensional parameter space (q_0, j_0) and y -redshift. Column (1): simulation identification in the text with the used data ($S = \text{SNeIa}$, $G = \text{GRBs}$, $H = \text{Hubble}$, $B = \text{BAO}$; the index (c) refers to the redshift-cut sub-sample, with $z < 1$) and the applied priors (we indicate the redshift range where positiveness of quantities described in § (V A) is applied). Columns (2) - (3) - (4): best fit estimations of cosmographic parameters with 1σ confidence level. Column (5): chi square and reduced chi square values. Columns (6) - (7) - (8) - (9): best fit estimations of dark energy (CPL) parameters with 1σ confidence level for the constant dark energy model and the dynamical one with fixed Ω_m as described in § (VI).

Data	Best fit parameters			CDE		DDE ($\Omega_m = 0.245$)	
S	q_0	j_0	χ^2 ($\chi^2/d.o.f.$)	Ω_m	w_0	w_0	w_a
$0 < y < 1$	$-0.668^{+0.047}_{-0.054}$	$0.414^{+0.394}_{-0.184}$	544.39 (0.983)	$0.066^{+0.085}_{-0.048}$	$-0.833^{+0.060}_{-0.114}$	$-1.032^{+0.042}_{-0.048}$	$-0.599^{+0.230}_{-0.111}$
$0 < y < 0.584$	$-0.664^{+0.047}_{-0.051}$	$0.373^{+0.360}_{-0.158}$	544.31 (0.982)	$0.056^{+0.079}_{-0.040}$	$-0.821^{+0.052}_{-0.103}$	$-1.028^{+0.041}_{-0.044}$	$-0.621^{+0.199}_{-0.097}$
$0 < y < 1^{(c)}$	$-0.646^{+0.052}_{-0.066}$	$0.375^{+0.524}_{-0.184}$	526.08 (0.985)	$0.069^{+0.109}_{-0.051}$	$-0.818^{+0.062}_{-0.150}$	$-1.012^{+0.046}_{-0.058}$	$-0.562^{+0.295}_{-0.121}$
$0 < y < 0.5^{(c)}$	$-0.648^{+0.053}_{-0.062}$	$0.392^{+0.490}_{-0.196}$	526.10 (0.985)	$0.073^{+0.103}_{-0.054}$	$-0.824^{+0.066}_{-0.143}$	$-1.014^{+0.047}_{-0.054}$	$-0.556^{+0.286}_{-0.124}$
S-G	q_0	j_0	χ^2 ($\chi^2/d.o.f.$)	Ω_m	w_0	w_0	w_a
$0 < y < 1$	$-0.671^{+0.054}_{-0.048}$	$0.405^{+0.400}_{-0.177}$	551.19 (0.885)	$0.063^{+0.084}_{-0.046}$	$-0.830^{+0.057}_{-0.114}$	$-1.034^{+0.043}_{-0.047}$	$-0.609^{+0.227}_{-0.107}$
$0 < y < 0.871$	$-0.669^{+0.046}_{-0.056}$	$0.400^{+0.391}_{-0.170}$	551.18 (0.885)	$0.062^{+0.083}_{-0.045}$	$-0.829^{+0.055}_{-0.112}$	$-1.032^{+0.041}_{-0.049}$	$-0.610^{+0.219}_{-0.108}$
$0 < y < 1^{(c)}$	$-0.643^{+0.052}_{-0.055}$	$0.357^{+0.383}_{-0.175}$	529.32 (0.957)	$0.064^{+0.089}_{-0.047}$	$-0.813^{+0.059}_{-0.114}$	$-1.009^{+0.046}_{-0.048}$	$-0.577^{+0.231}_{-0.108}$
$0 < y < 0.5^{(c)}$	$-0.645^{+0.052}_{-0.062}$	$0.372^{+0.487}_{-0.188}$	529.33 (0.957)	$0.068^{+0.18}_{-0.050}$	$-0.817^{+0.064}_{-0.144}$	$-1.011^{+0.046}_{-0.055}$	$-0.567^{+0.291}_{-0.115}$
S-H	q_0	j_0	χ^2 ($\chi^2/d.o.f.$)	Ω_m	w_0	w_0	w_a
$0 < y < 1$	$-0.924^{+0.250}_{-0.190}$	$3.535^{+2.022}_{-2.478}$	589.03 (1.041)	$0.402^{+0.046}_{-0.171}$	$-1.594^{+0.577}_{-0.353}$	$-1.258^{+0.223}_{-0.169}$	$1.263^{+0.964}_{-1.319}$
$0 < y < 0.638$	$-0.905^{+0.255}_{-0.202}$	$3.360^{+2.116}_{-2.532}$	589.24 (1.041)	$0.397^{+0.049}_{-0.205}$	$-1.560^{+0.610}_{-0.369}$	$-1.241^{+0.225}_{-0.179}$	$1.169^{+1.014}_{-1.368}$
$0 < y < 1^{(c)}$	$-0.640^{+0.049}_{-0.065}$	$0.365^{+0.512}_{-0.180}$	528.60 (0.975)	$0.070^{+0.108}_{-0.051}$	$-0.814^{+0.060}_{-0.148}$	$-1.006^{+0.043}_{-0.056}$	$-0.555^{+0.291}_{-0.121}$
$0 < y < 0.5^{(c)}$	$-0.642^{+0.054}_{-0.067}$	$0.391^{+0.531}_{-0.206}$	528.63 (0.975)	$0.077^{+0.113}_{-0.057}$	$-0.823^{+0.070}_{-0.159}$	$-1.009^{+0.048}_{-0.060}$	$-0.542^{+0.321}_{-0.127}$
S-G-H	q_0	j_0	χ^2 ($\chi^2/d.o.f.$)	Ω_m	w_0	w_0	w_a
$0 < y < 1$	$-0.878^{+0.237}_{-0.202}$	$3.036^{+2.122}_{-2.298}$	597.09 (0.940)	$0.382^{+0.058}_{-0.206}$	$-1.492^{+0.567}_{-0.388}$	$-1.217^{+0.209}_{-0.178}$	$0.991^{+1.032}_{-1.248}$
$0 < y < 0.871$	$-0.891^{+0.232}_{-0.188}$	$3.178^{+1.947}_{-2.264}$	596.89 (0.940)	$0.389^{+0.052}_{-0.180}$	$-1.521^{+0.545}_{-0.354}$	$-1.228^{+0.204}_{-0.165}$	$1.071^{+0.956}_{-1.215}$
$0 < y < 1^{(c)}$	$-0.642^{+0.051}_{-0.060}$	$0.386^{+0.473}_{-0.197}$	531.88 (0.948)	$0.075^{+0.102}_{-0.054}$	$-0.821^{+0.065}_{-0.139}$	$-1.009^{+0.045}_{-0.053}$	$-0.547^{+0.280}_{-0.125}$
$0 < y < 0.5^{(c)}$	$-0.645^{+0.053}_{-0.063}$	$0.395^{+0.529}_{-0.201}$	531.88 (0.948)	$0.077^{+0.108}_{-0.055}$	$-0.824^{+0.067}_{-0.153}$	$-1.011^{+0.047}_{-0.055}$	$-0.543^{+0.303}_{-0.125}$
S-G-H-B	q_0	j_0	χ^2 ($\chi^2/d.o.f.$)	Ω_m	w_0	w_0	w_a
$0 < y < 1$	$-0.932^{+0.186}_{-0.169}$	$3.580^{+1.824}_{-1.850}$	597.22 (0.939)	$0.402^{+0.043}_{-0.099}$	$-1.602^{+0.407}_{-0.312}$	$-1.265^{+0.164}_{-0.148}$	$1.273^{+0.856}_{-0.964}$
$0 < y < 0.871$	$-0.923^{+0.200}_{-0.179}$	$3.479^{+1.911}_{-1.965}$	597.29 (0.939)	$0.399^{+0.046}_{-0.121}$	$-1.581^{+0.451}_{-0.333}$	$-1.256^{+0.178}_{-0.157}$	$1.220^{+0.916}_{-1.057}$
$0 < y < 1^{(c)}$	$-0.645^{+0.053}_{-0.064}$	$0.392^{+0.527}_{-0.207}$	532.53 (0.947)	$0.075^{+0.105}_{-0.055}$	$-0.823^{+0.068}_{-0.146}$	$-1.011^{+0.046}_{-0.055}$	$-0.548^{+0.292}_{-0.124}$
$0 < y < 0.5^{(c)}$	$-0.641^{+0.049}_{-0.061}$	$0.360^{+0.479}_{-0.175}$	532.50 (0.947)	$0.067^{+0.106}_{-0.050}$	$-0.813^{+0.059}_{-0.141}$	$-1.007^{+0.043}_{-0.054}$	$-0.563^{+0.279}_{-0.115}$
S-H-B	q_0	j_0	χ^2 ($\chi^2/d.o.f.$)	Ω_m	w_0	w_0	w_a
$0 < y < 1$	$-0.940^{+0.240}_{-0.177}$	$3.688^{+1.917}_{-2.377}$	589.62 (1.040)	$0.405^{+0.043}_{-0.149}$	$-1.623^{+0.545}_{-0.323}$	$-1.271^{+0.216}_{-0.155}$	$1.319^{+0.911}_{-1.266}$
$0 < y < 0.871$	$-0.912^{+0.259}_{-0.196}$	$3.390^{+2.097}_{-2.564}$	597.29 (0.939)	$0.397^{+0.050}_{-0.199}$	$-1.564^{+0.610}_{-0.374}$	$-1.247^{+0.228}_{-0.173}$	$1.184^{+1.023}_{-1.366}$
$0 < y < 1^{(c)}$	$-0.644^{+0.052}_{-0.060}$	$0.387^{+0.450}_{-0.198}$	529.27 (0.975)	$0.073^{+0.096}_{-0.054}$	$-0.822^{+0.066}_{-0.129}$	$-1.010^{+0.046}_{-0.052}$	$-0.553^{+0.258}_{-0.120}$
$0 < y < 0.5^{(c)}$	$-0.644^{+0.053}_{-0.065}$	$0.381^{+0.526}_{-0.196}$	529.26 (0.975)	$0.072^{+0.108}_{-0.054}$	$-0.820^{+0.066}_{-0.151}$	$-1.010^{+0.047}_{-0.057}$	$-0.554^{+0.299}_{-0.122}$

Table IV. Results in the three dimensional parameter space (q_0, j_0, s_0) and y -redshift. Void rows correspond to MCMC which do not pass the convergence test. Column (1): simulation identification in the text with the used data ($S = \text{SNeIa}$, $G = \text{GRBs}$, $H = \text{Hubble}$, $B = \text{BAO}$; the index (c) refers to the redshift-cut sub-sample, with $z < 1$) and the applied priors (we indicate the redshift range where positiveness of quantities described in § (VA) is applied). Columns (2) - (3) - (4): best fit estimations of cosmographic parameters with 1σ confidence level. Column (5): chi square and reduced chi square values. Columns (6) - (7) - (8): best fit estimations of dark energy (CPL) parameters with 1σ confidence level for the dynamical dark energy model as described in § (VI).

Data	Best fit parameters				DDE		
S	q_0	j_0	s_0	$\chi^2 (\chi^2/d.o.f.)$	Ω_m	w_0	w_a
$0 < y < 1$	$-0.498^{+0.048}_{-0.074}$	$0.105^{+0.452}_{-0.129}$	$-0.053^{+0.130}_{-0.464}$	542.51 (0.981)	$0.066^{+0.121}_{-0.046}$	$-0.711^{+0.054}_{-0.156}$	$0.007^{+0.073}_{-0.140}$
$0 < y < 0.584$	$-0.494^{+0.047}_{-0.066}$	$0.091^{+0.373}_{-0.128}$	$-0.080^{+0.116}_{-0.398}$	542.55 (0.981)	$0.059^{+0.114}_{-0.040}$	$-0.703^{+0.049}_{-0.141}$	$0.002^{+0.067}_{-0.126}$
$0 < y < 1^{(c)}$	$-0.502^{+0.054}_{-0.082}$	$0.134^{+0.540}_{-0.160}$	$-0.056^{+0.141}_{-0.479}$	525.63 (0.986)	$0.073^{+0.146}_{-0.052}$	$-0.720^{+0.062}_{-0.192}$	$0.007^{+0.074}_{-0.181}$
$0 < y < 0.5^{(c)}$	$-0.498^{+0.054}_{-0.074}$	$0.093^{+0.439}_{-0.150}$	$-0.068^{+0.155}_{-0.680}$	525.68 (0.986)	$0.069^{+0.146}_{-0.049}$	$-0.714^{+0.058}_{-0.186}$	$0.0009^{+0.0788}_{-0.2164}$
S-G	q_0	j_0	s_0	$\chi^2 (\chi^2/d.o.f.)$	Ω_m	w_0	w_a
$0 < y < 1$	$-0.501^{+0.050}_{-0.079}$	$0.130^{+0.520}_{-0.157}$	$-0.063^{+0.151}_{-0.511}$	549.00 (0.883)	$0.079^{+0.121}_{-0.056}$	$-0.724^{+0.062}_{-0.167}$	$0.006^{+0.071}_{-0.168}$
$0 < y < 0.871$	—	—	—	—	—	—	—
$0 < y < 1^{(c)}$	$-0.501^{+0.051}_{-0.073}$	$0.146^{+0.483}_{-0.159}$	$-0.038^{+0.215}_{-0.335}$	528.94 (0.958)	$0.070^{+0.112}_{-0.049}$	$-0.718^{+0.057}_{-0.148}$	$0.014^{+0.071}_{-0.124}$
$0 < y < 0.5^{(c)}$	$-0.496^{+0.053}_{-0.079}$	$0.098^{+0.517}_{-0.135}$	$-0.039^{+0.191}_{-0.510}$	529.00 (0.958)	$0.068^{+0.143}_{-0.050}$	$-0.711^{+0.057}_{-0.195}$	$0.003^{+0.073}_{-0.176}$
S-H	q_0	j_0	s_0	$\chi^2 (\chi^2/d.o.f.)$	Ω_m	w_0	w_a
$0 < y < 1$	—	—	—	—	—	—	—
$0 < y < 0.638$	—	—	—	—	—	—	—
$0 < y < 1^{(c)}$	$-0.497^{+0.051}_{-0.073}$	$0.102^{+0.480}_{-0.134}$	$-0.076^{+0.138}_{-0.420}$	527.28 (0.975)	$0.067^{+0.126}_{-0.047}$	$-0.711^{+0.055}_{-0.157}$	$0.002^{+0.069}_{-0.141}$
$0 < y < 0.5^{(c)}$	$-0.497^{+0.053}_{-0.076}$	$0.105^{+0.497}_{-0.150}$	$-0.066^{+0.151}_{-0.479}$	527.29 (0.975)	$0.070^{+0.132}_{-0.050}$	$-0.714^{+0.058}_{-0.171}$	$0.002^{+0.077}_{-0.162}$
S-G-H	q_0	j_0	s_0	$\chi^2 (\chi^2/d.o.f.)$	Ω_m	w_0	w_a
$0 < y < 1$	—	—	—	—	—	—	—
$0 < y < 0.871$	—	—	—	—	—	—	—
$0 < y < 1^{(c)}$	$-0.493^{+0.048}_{-0.067}$	$0.079^{+0.414}_{-0.118}$	$-0.073^{+0.115}_{-0.448}$	530.65 (0.948)	$0.058^{+0.119}_{-0.041}$	$-0.701^{+0.050}_{-0.140}$	$-0.001^{+0.070}_{-0.131}$
$0 < y < 0.5^{(c)}$	$-0.498^{+0.052}_{-0.076}$	$0.128^{+0.479}_{-0.157}$	$-0.051^{+0.119}_{-0.389}$	530.58 (0.947)	$0.066^{+0.126}_{-0.047}$	$-0.710^{+0.056}_{-0.163}$	$0.012^{+0.071}_{-0.146}$
S-G-H-B	q_0	j_0	s_0	$\chi^2 (\chi^2/d.o.f.)$	Ω_m	w_0	w_a
$0 < y < 1$	—	—	—	—	—	—	—
$0 < y < 0.871$	$-0.675^{+0.124}_{-0.115}$	$1.244^{+0.842}_{-1.248}$	$-0.098^{+0.219}_{-15.996}$	572.41 (0.901)	$0.364^{+0.087}_{-0.117}$	$-1.272^{+0.312}_{-0.205}$	$-0.326^{+0.352}_{-2.416}$
$0 < y < 1^{(c)}$	$-0.497^{+0.050}_{-0.069}$	$0.100^{+0.406}_{-0.131}$	$-0.058^{+0.143}_{-0.457}$	531.52 (0.947)	$0.065^{+0.123}_{-0.046}$	$-0.714^{+0.058}_{-0.151}$	$0.004^{+0.071}_{-0.154}$
$0 < y < 0.5^{(c)}$	$-0.503^{+0.052}_{-0.070}$	$0.134^{+0.455}_{-0.158}$	$-0.041^{+0.151}_{-0.423}$	531.49 (0.947)	$0.067^{+0.107}_{-0.047}$	$-0.716^{+0.056}_{-0.129}$	$0.016^{+0.074}_{-0.144}$
S-H-B	q_0	j_0	s_0	$\chi^2 (\chi^2/d.o.f.)$	Ω_m	w_0	w_a
$0 < y < 1$	—	—	—	—	—	—	—
$0 < y < 0.638$	—	—	—	—	—	—	—
$0 < y < 1^{(c)}$	$-0.506^{+0.055}_{-0.078}$	$0.132^{+0.517}_{-0.169}$	$-0.105^{+0.162}_{-0.787}$	528.17 (0.974)	$0.084^{+0.136}_{-0.061}$	$-0.730^{+0.069}_{-0.183}$	$-0.006^{+0.086}_{-0.216}$
$0 < y < 0.5^{(c)}$	$-0.509^{+0.054}_{-0.085}$	$0.138^{+0.578}_{-0.170}$	$-0.058^{+0.148}_{-0.687}$	528.21 (0.975)	$0.086^{+0.148}_{-0.060}$	$-0.733^{+0.068}_{-0.205}$	$-0.00004^{+0.08549}_{-0.23504}$

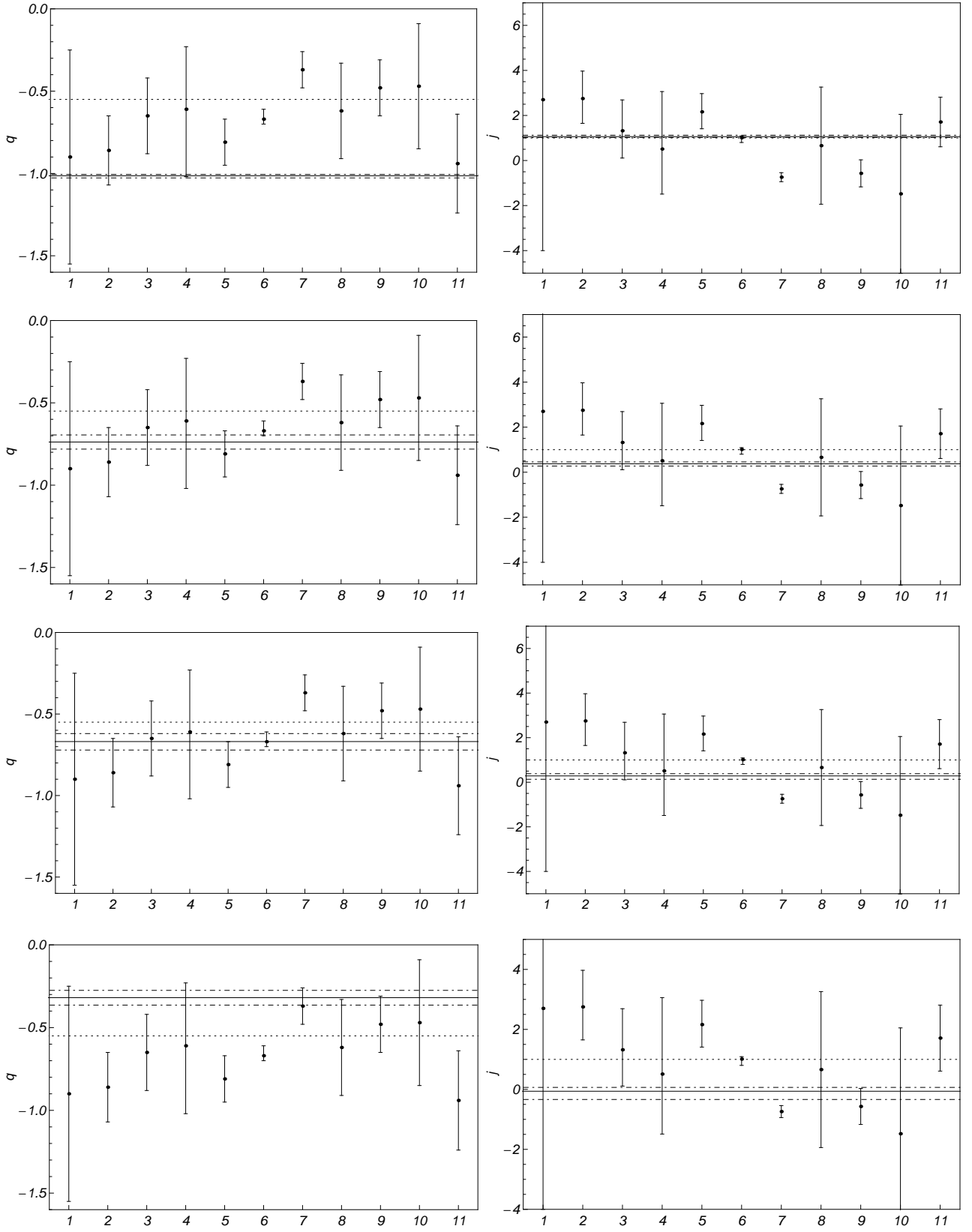


Figure 5. Comparing deceleration and jerk values from the literature with results from: (*First panel.*) SNeIa only, two dimensional cosmography and prior on z -redshift range $z > 0$; (*Second panel.*) SNeIa only, two dimensional cosmography and prior on z -redshift range $z < 1.4$; (*Third panel.*) cut SNeIa only, two dimensional cosmography and prior on z -redshift range $z < 1$; (*Fourth panel.*) cut SNeIa only, three dimensional cosmography and prior on z -redshift range $z > 0$. References in numerical order as they appear in the figure: (1) - John (2004); (2) - Rapetti (2006), Gold SN subsample; (3) - Rapetti (2006), Legacy SN subsample; (4) - Rapetti (2006), X-ray clusters subsample; (5) - Rapetti (2006), all subsamples; (6) - Poplawski (2006); (7) - Cattoen (2007), Gold SN in z -redshift; (8) - Cattoen (2007), Gold SN in y -redshift; (9) - Cattoen (2007), Legacy SN in z -redshift; (10) - Cattoen (2007), Legacy SN in y -redshift; (11) - Capozziello, Izzo (2008). Solid horizontal line is our best fit result; dotted horizontal line shows its 1σ confidence level; dashed horizontal line shows Λ CDM expectation.

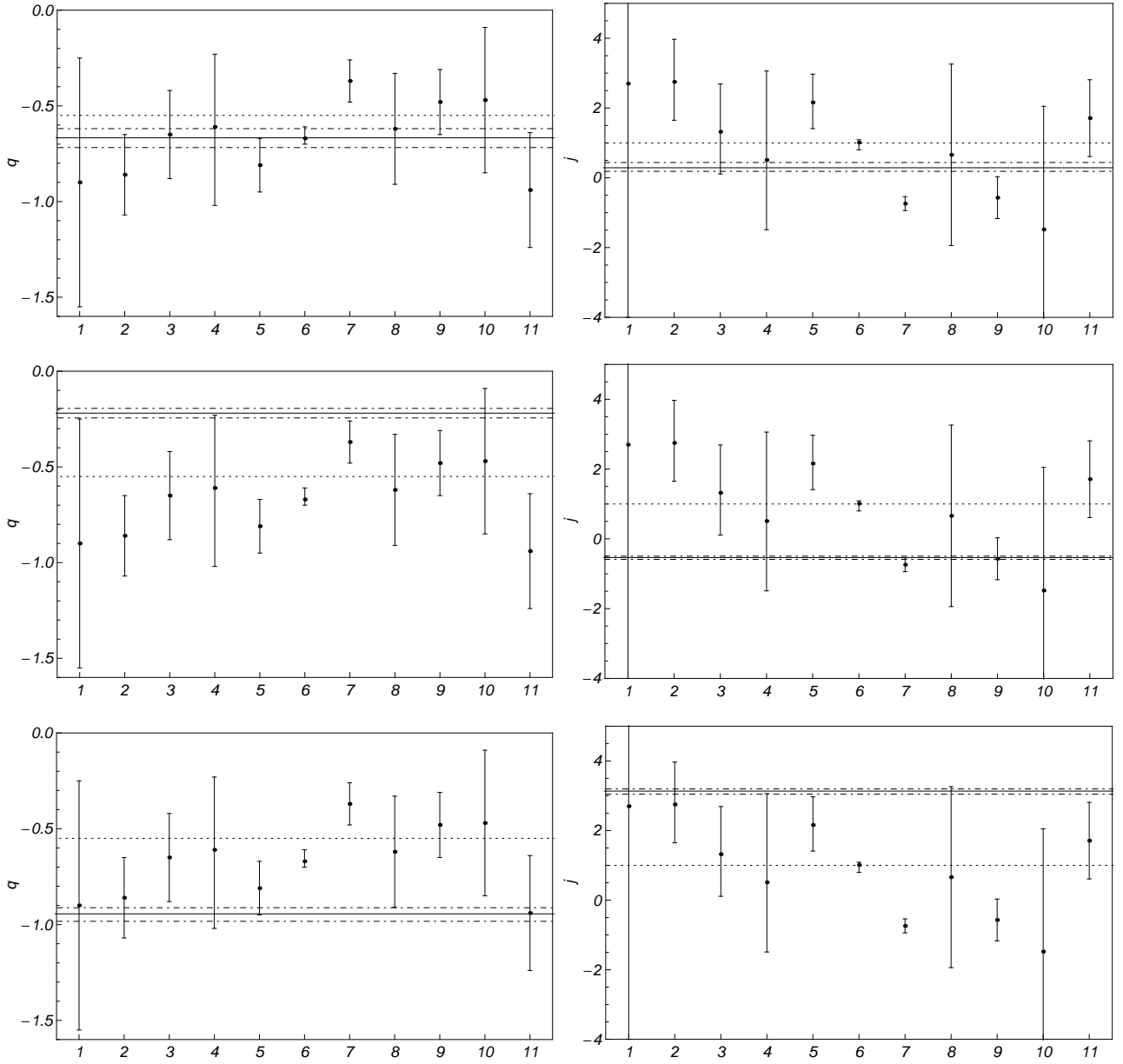


Figure 6. Comparing deceleration and jerk values from the literature with results from: (*First panel.*) all cut data, two dimensional cosmography and prior on z -redshift range $z < 1$; (*Second panel.*) SNeIa and Hubble data, three dimensional cosmography and prior on z -redshift range $z > 0$; (*Third panel.*) SNeIa and Hubble data, three dimensional cosmography and prior on z -redshift range $z < 1.76$. References in numerical order as the appear in the figure: (1) - John (2004); (2) - Rapetti (2006), Gold SN subsample; (3) - Rapetti (2006), Legacy SN subsample; (4) - Rapetti (2006), X-ray clusters subsample; (5) - Rapetti (2006), all subsamples; (6) - Poplawski (2006); (7) - Cattoen (2007), Gold SN in z -redshift; (8) - Cattoen (2007), Gold SN in y -redshift; (9) - Cattoen (2007), Legacy SN in z -redshift; (10) - Cattoen (2007), Legacy SN in y -redshift; (11) - Capozziello, Izzo (2008). Solid horizontal line is our best fit result; dotted horizontal lines show its 1σ confidence level; dashed horizontal line shows Λ CDM expectation.

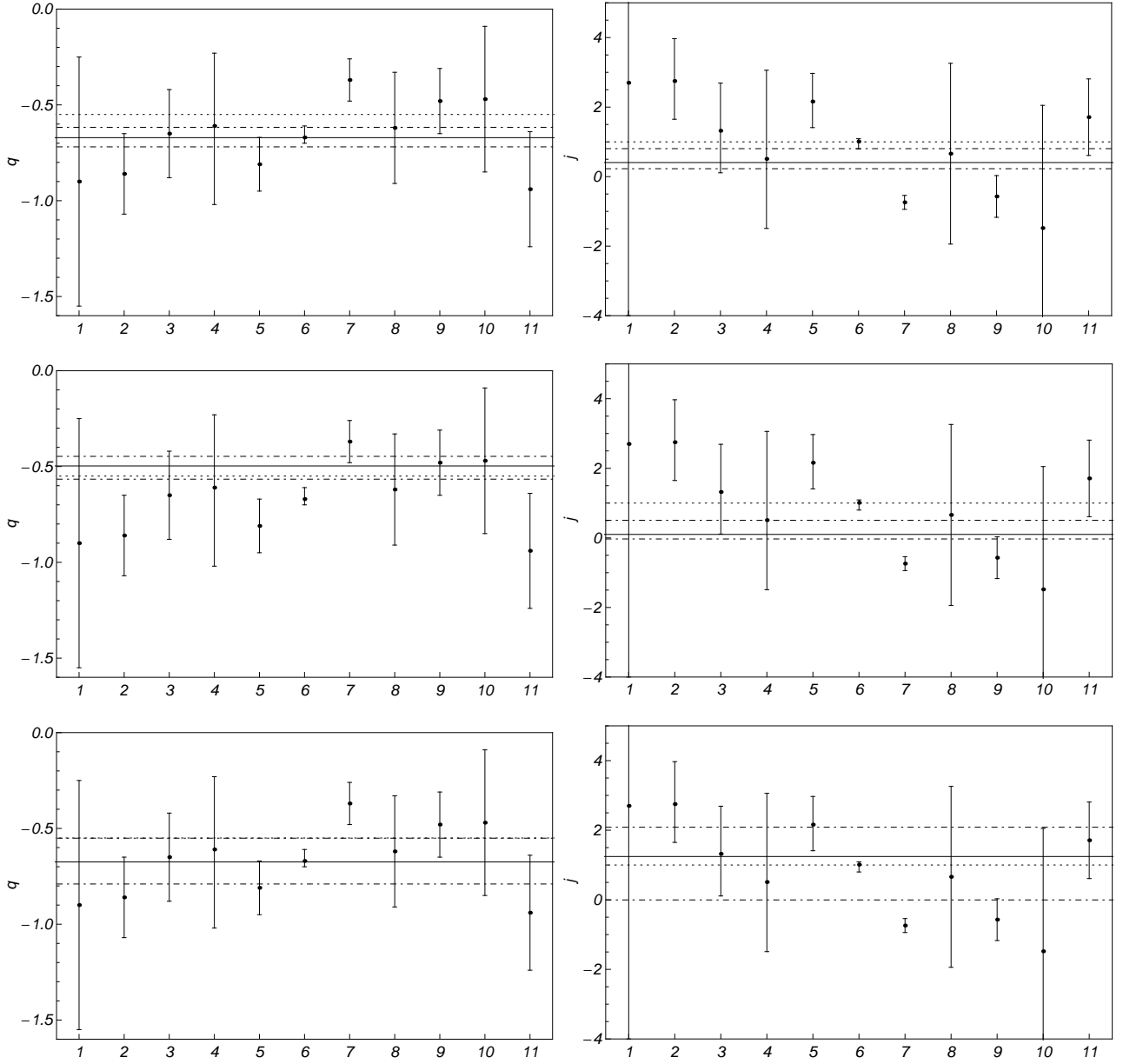


Figure 7. Comparing deceleration and jerk values from the literature with results from: (*First panel.*) SNeIa data, two dimensional cosmography and prior on y -redshift range $0 < y < 1$; (*Second panel.*) all data, three dimensional cosmography and prior on y -redshift range $0 < y < 1$; (*Third panel.*) all data, three dimensional cosmography and prior on y -redshift range $0 < y < 0.871$. References in numerical order as the appear in the figure: (1) - John (2004); (2) - Rapetti (2006), Gold SN subsample; (3) - Rapetti (2006), Legacy SN subsample; (4) - Rapetti (2006), X-ray clusters subsample; (5) - Rapetti (2006), all subsamples; (6) - Poplawski (2006); (7) - Cattoen (2007), Gold SN in z -redshift; (8) - Cattoen (2007), Gold SN in y -redshift; (9) - Cattoen (2007), Legacy SN in z -redshift; (10) - Cattoen (2007), Legacy SN in y -redshift; (11) - Capozziello, Izzo (2008). Solid horizontal line is our best fit result; dotdashed horizontal lines show its 1σ confidence level; dotted horizontal line shows Λ CDM expectation.